nature communications

Article

https://doi.org/10.1038/s41467-025-58371-8

Multilayered HIV-1 resistance in HSPCs through *CCR5* Knockout and B cell secretion of HIV-inhibiting antibodies

Received: 22 February 2024

Accepted: 19 March 2025

Published online: 01 April 2025

Check for updates

William N. Feist[1,2,10], Sofia E. Luna[1,2,3,10], Kaya Ben-Efraim[2], Maria V. Filsinger Interrante[3,4,5], Alvaro Amorin[1,2,3], Nicole M. Johnston[2], Theodora U. J. Bruun[5,6], Ashley Utz[3,4], Hana Y. Ghanim[1,2], Benjamin J. Lesch[2,7,8], Theresa M. McLaughlin[9], Amanda M. Dudek[1,2] ✉ & Matthew H. Porteus[1,2] ✉

Allogeneic transplantation of *CCR5* null hematopoietic stem and progenitor cells (HSPCs) is the only known cure for HIV-1 infection. However, this treatment is limited because of the rarity of *CCR5*-null matched donors, the morbidities associated with allogeneic transplantation, and the prevalence of HIV-1 strains resistant to *CCR5* knockout (KO) alone. Here, we propose a one-time therapy through autologous transplantation of HSPCs genetically engineered ex vivo to produce both *CCR5* KO cells and long-term secretion of potent HIV-1 inhibiting antibodies from B cell progeny. CRISPR-Cas9-engineered HSPCs engraft and reconstitute multiple hematopoietic lineages in vivo and can be engineered to express multiple antibodies simultaneously (in pre-clinical models). Human B cells engineered to express each antibody secrete neutralizing concentrations capable of inhibiting HIV-1 pseudovirus infection in vitro. This work lays the foundation for a potential one-time functional cure for HIV-1 through combining the long-term delivery of therapeutic antibodies against HIV-1 and the known efficacy of *CCR5* KO HSPC transplantation.

There are 39 million people worldwide living with HIV infection[1]. While great advances in small-molecule antiretroviral therapy (ART) have resulted in combination drug regimens that can control viral loads, in 2022 alone there were over 600,000 AIDS-related deaths, underlining that HIV remains a global epidemic with substantial morbidity and mortality[1–3]. This is due in part to the strict adherence necessary for ART to remain effective[4–6]. Current regimens call for lifetime daily dosing to suppress long-term viral reservoirs and prevent viral rebound[7,8]. Because of this, significant research efforts have sought to identify novel treatment modalities that provide a more durable long-term cure.

The discovery of highly potent HIV-1 inhibiting antibodies with relatively long half-lives has led to numerous clinical trials for sustained control of HIV-1[9,10]. The first monoclonal antibody clinically approved to treat HIV-1, Ibalizumab, acts as a post-attachment inhibitor by binding HIV-1's primary receptor on human cells, CD4[11–14]. In addition to this, numerous potent antibodies that act against diverse HIV-1 subtypes have been identified to bind and neutralize HIV-1 directly[15,16]. These antibodies, known as broadly neutralizing antibodies (bNAbs), target highly conserved regions of the viral envelope to inhibit infection. Recent and ongoing trials are testing the efficacy of

[1]Institute for Stem Cell Biology & Regenerative Medicine, Stanford University School of Medicine, Stanford, CA, USA. [2]Department of Pediatrics, Stanford University School of Medicine, Stanford, CA, USA. [3]Stanford Medical Scientist Training Program, Stanford University School of Medicine, Stanford, CA, USA. [4]Stanford Biophysics Program, Stanford University School of Medicine, Stanford, CA, USA. [5]Stanford ChEM-H, Stanford University, Stanford, CA, USA. [6]Department of Biochemistry, Stanford University School of Medicine, Stanford, CA, USA. [7]Department of Surgery, University of California, San Francisco, San Francisco, CA, USA. [8]Eli and Edythe Broad Center for Regeneration Medicine, University of California, San Francisco, San Francisco, CA, USA. [9]Stanford University Mass Spectrometry, Stanford University, Stanford, CA, USA. [10]These authors contributed equally: William N. Feist, Sofia E. Luna.
✉e-mail: amanda-dudek@uiowa.edu; mporteus@stanford.edu

targeting multiple envelope epitopes simultaneously to prevent the generation of resistance mutations[9,10,17–19]. These trials have shown that bNAbs can maintain viral suppression and prevent the formation of escape mutants so long as antibody titers remain above a therapeutic threshold. While the longer half-life of antibodies does allow for reduced frequency of dosing, lifelong repeated administration would still be required to maintain efficacy.

One promising method for sustained delivery of bNAbs is through AAV-mediated delivery of antibody expression cassettes, known as vectored immunoprophylaxis[20–25]. Trials in mice, macaques, and recently humans have demonstrated the potential of this strategy for sustained secretion of therapeutic anti-HIV-1 antibodies. However, pre-existing immunity against AAV vectors, low levels of antibody secretion, uncertainty regarding long-term expression, and seroconversion preventing re-dosing remain challenges limiting this approach[26,27]. Another potential method for long-term maintenance of antibody expression is the direct editing of autologous B cells. B cells can be directly engineered for custom antibody expression from the B cell receptor locus, allowing for participation of the custom antibody in the humoral immune response[28–32]. However, there is currently no clinical protocol for the engraftment of B cells in patients and it remains unclear how long they may persist in the body.

Hematopoietic stem cell transplantation (HSCT) of *CCR5* knockout (KO) cells is the only reported long-term functional cure for HIV-1 infection. Demonstrated first in the cases of the Berlin and London patients, allogeneic HSCT with cells from donors carrying the naturally occurring *CCR5-Δ32* KO mutation resulted in reconstitution with cells that were resistant to their CCR5-tropic (R5-tropic) HIV-1[33,34]. After treatment interruption of ART, each patient maintained viral suppression and was considered functionally cured of their infection. While this strategy has shown continued success, it is not widely available to the vast majority of patients[35]. The rarity of identifying a *CCR5* KO matched donor and the morbidities associated with allogeneic transplantation, such as graft versus host disease (GvHD), limit this treatment to only a small fraction of patients who require HSCT for an underlying malignancy[36–38]. Moreover, HSCT with *CCR5* KO cells is ineffective in patients carrying CXCR4-tropic (X4-tropic) HIV-1 strains that do not rely on CCR5 for cellular entry. This was demonstrated in the case of the Essen patient, where *CCR5* KO HSCT followed by ART interruption resulted in rebound of X4-tropic virus[39]. X4-tropic HIV-1 is estimated to be present in 18% to 52% of patients, highlighting the need for strategies to combat these strains[40,41].

Autologous HSCT with genetically modified cells is a promising strategy to overcome the risk of GvHD and the need for rare donor cells. One recent trial demonstrated the feasibility of autologous transplantation of cells genetically modified for *CCR5* KO in a patient with HIV-1[42]. However, low editing rates resulted in a failure to prevent viral rebound, underscoring the importance of efficient modification to minimize viral replication in unedited cells. Other strategies have modified hematopoietic stem and progenitor cells (HSPCs) with *CCR5* KO, lentiviral delivery of HIV-1 inhibiting proteins, neutralizing antibodies, and inhibitory RNAs against *CCR5* and viral targets[42–48]. Several of these strategies benefit from layering multiple methods of HIV-1 inhibition to control both R5-tropic and X4-tropic HIV-1, however, limited editing efficiency and the risk of malignancy resulting from insertional mutagenesis have hampered their application[49]. Meanwhile, advances in precision gene editing with CRISPR-Cas9 have allowed for high-efficiency cellular engineering without the risks associated with lentiviral integration. Moreover, the clinical approval of Casgevy for the treatment of sickle cell disease and beta-thalassemia has demonstrated that CRISPR-Cas9 engineered HSPCs can engraft and generate multi-lineage reconstitution, encouraging further application of CRISPR-edited autologous HSCT[50]. Recently, we reported a CRISPR-Cas9-based strategy in HSPCs for simultaneous KO out of *CCR5* with knock-in of expression cassettes for two HIV-1 inhibiting proteins[51]. While this work demonstrated the feasibility of high-efficiency editing to deliver multilayered genetic resistance to HIV-1, it relies on a cell-autonomous resistance scheme that leaves unedited cells vulnerable to infection. As such, we seek to develop a strategy that can deliver both cell-intrinsic and cell-extrinsic protection to inhibit infection in both edited and unedited cells.

Here, we seek to combine the success of *CCR5* KO HSCT with the potency of sustained antibody therapy through a simultaneous knockout knock-in gene editing strategy in HSPCs. Our system is designed to deliver broad resistance against R5-tropic HIV-1 through *CCR5* KO and to include additional layers of non-cell-autonomous protection through the secretion of multiple HIV-1 inhibiting antibodies that act broadly against both R5- and X4-tropic viruses. To combat the formation of escape mutants, our system employs multiple well-established antibodies targeting diverse epitopes. In this study, we demonstrate that HSPCs can be efficiently edited at the *CCR5* locus for knock-in of multiple HIV-1 inhibiting antibody expression cassettes. Importantly, these engineered HSPCs engraft and demonstrate multilineage potential following transplantation in immunodeficient mice. Moreover, we show that primary human B cells carrying the antibody expression cassettes secrete neutralizing levels of antibodies in vitro. Overall, this work establishes a strategy for autologous transplantation of HSPCs modified for long-term secretion of therapeutic antibodies from B cell progeny.

Results

HIV-1 inhibiting antibodies maintain function with a peptide linker

Recent trials investigating direct injection of anti-HIV-1 antibodies to control disease highlight the need to use multiple antibodies targeting different epitopes in combination to prevent viral escape[17–19]. To this end, we utilize well-established antibodies that are known to inhibit R5-tropic and X4-tropic HIV-1. These antibodies include the clinically approved antibody Ibalizumab and several bNAbs that target different highly conserved regions of the HIV-1 envelope: 10-1074 (V3 Loop), PGDM1400 (V1/2 Loop), CAP256V2LS (V1/2 Loop), 3BNC117 (CD4 binding site), and 1-18 (CD4 binding site) (Supplementary Table 1)[52–56].

While traditional production of these IgG antibodies involves transfection of cell culture with two separate plasmids encoding the IgG heavy and light chain, our delivery system necessitates the antibody components be delivered as a single transcript for knock-in to the *CCR5* locus. However, expression from B cell progeny that are producing antibodies from the native immunoglobulin loci may result in mispairing of therapeutic antibodies with endogenous heavy or light chains, resulting in dysfunctional epitope recognition. For this reason, we employed a linker system to physically pair the therapeutic antibody heavy and light chain to mitigate the risk for mispairing and the potential formation of deleterious antibody products (Fig. 1a and Supplementary Table 2)[57].

To determine if the addition of the linker impacts function, each antibody was produced in the conventional manner from a separate cassette for the light and heavy chains (traditional antibody) and from a single cassette with a linker pairing the light and heavy chains (linker antibody) (Fig. 1a and Supplementary Fig. 1a). Purified antibodies were analyzed with total protein SDS-PAGE analysis to determine production purity (Supplementary Fig. 1b) and with western blot analysis staining for IgG to show linkage of the light and heavy chains (Fig. 1b). Traditional antibodies were detected at the expected mass for a heavy chain alone at approximately 50 kDa, while linker antibodies formed a band with an expected higher molecular weight at 80 kDa, corresponding to the increased mass of the linker and light chain paired with the heavy chain (Fig. 1b). Next, each antibody was tested against a previously defined panel of HIV-1 pseudoviruses representing the global diversity of HIV-1 (Supplementary Table 3) in a TZM-bl infection assay to ensure neutralization potency was preserved with the added

https://doi.org/10.1038/s41467-025-58371-8

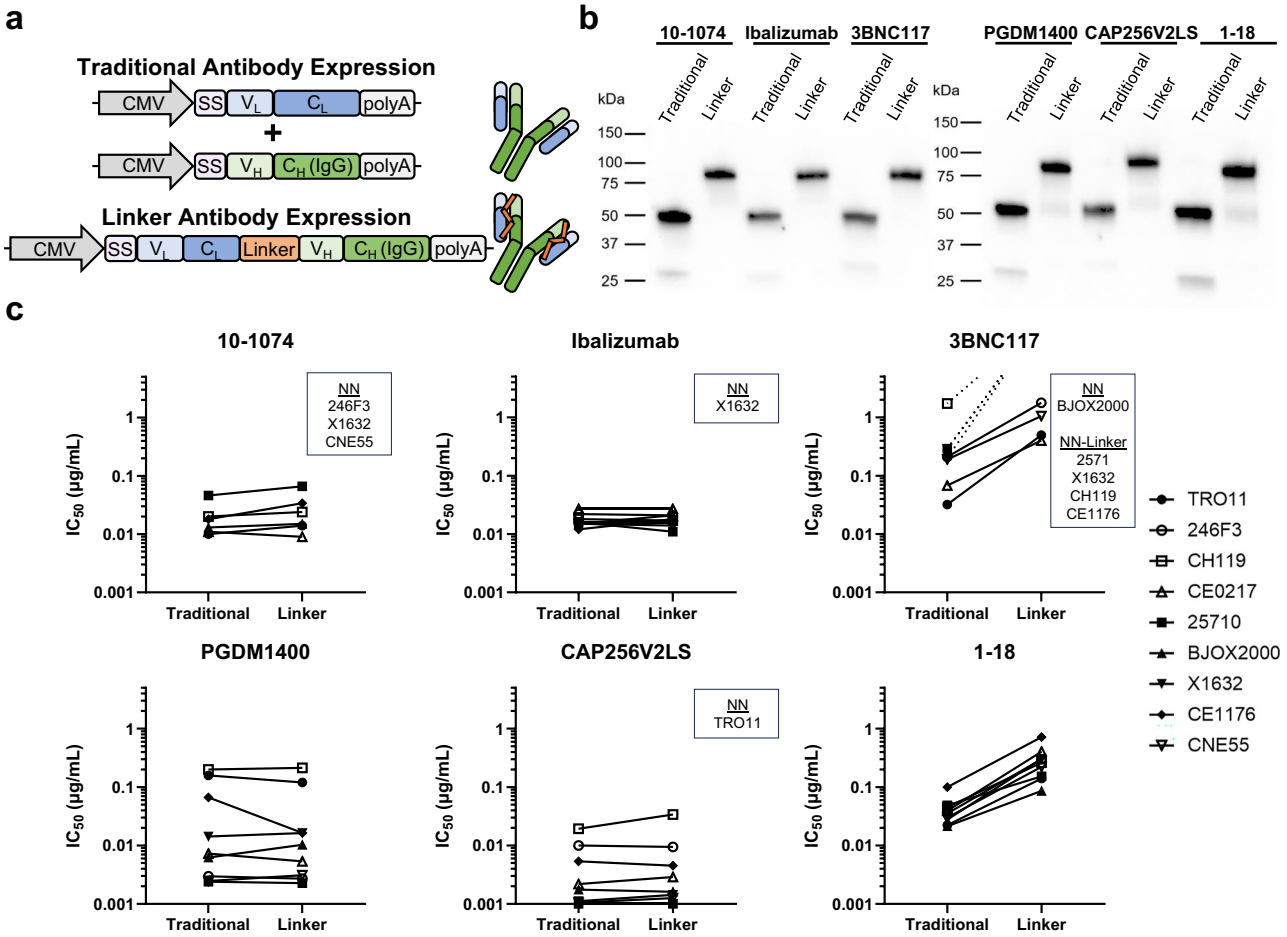

Fig. 1 | HIV inhibiting antibodies maintain function with a peptide linker. **a** Diagram of antibody expression with and without a peptide linker driven by the cytomegalovirus (CMV) promoter. **b** SDS-PAGE western blot of purified traditional and linker antibodies. **c** IC_{50} of traditional and linker antibodies against a panel of HIV-1 pseudoviruses measured in vitro with TZM-bl infection assay (IC_{50} was calculated from technical duplicate infections across serial dilutions of each antibody). Dotted lines indicate the linker antibody did not inhibit infection within the tested antibody concentrations (≤5 μg/mL) for a given pseudovirus. Pseudoviruses listed in each inset were not inhibited within the tested antibody concentrations (≤5 μg/mL) by both the traditional and linker antibody (NN) or the linker antibody only (NN-Linker). Source data are provided as a Source Data file.

linker[58,59]. The traditional IgG and linker versions of 10-1074, Ibalizumab, PGDM1400, and CAP256V2LS show comparable efficacy as demonstrated by measured half-maximal inhibitory concentration (IC_{50}) for each pseudovirus (Fig. 1c and Supplementary Table 4). Two antibodies, 3BNC117 and 1-18, demonstrated a marked reduction in neutralization efficacy when expressed with a peptide linker. Interestingly, these two antibodies both target the CD4 binding site on HIV-1, indicating that further optimization may be needed to employ a linker for this subset of antibodies. Overall, these results demonstrate that HIV-1 inhibiting antibodies can maintain function when expressed from a single transcript with a peptide linker physically pairing the light and heavy chains.

Simultaneous *CCR5* KO and antibody cassette knock-in in $CD34^+$ HSPCs

The modification of $CD34^+$ HSPCs is a promising strategy to deliver long-term HIV-1 treatment through hematopoietic reconstitution with resistant cells. However, high-efficiency editing is needed to mitigate the potential for escape mutants to form in non-edited cells and to deliver therapeutically relevant antibody levels. To this end, we employ CRISPR-Cas9 editing with electroporation of ribonucleoprotein (RNP) followed by adeno-associated virus serotype 6 (AAV6) delivery of DNA donor templates for knock-in by homology directed repair (HDR). *CCR5* KO is achieved with a highly efficient single guide RNA (sgRNA), sg-*CCR5*, we previously demonstrated to induce KO INDELs (Supplementary Fig. 2a) that confer resistance to R5-tropic HIV-1 infection in primary $CD4^+$ T cells[51]. We employ a high-fidelity version of Cas9 to minimize the potential of off-target INDELs, and previously performed amplicon deep sequencing off-target analysis with sg-*CCR5* showed it to be specific with no measurable off-target INDEL formation across the top 7 most likely off-target sites predicted in silico[51,60]. To further characterize the off-target potential of this sgRNA, we performed amplicon deep sequencing of the next highest ranked off-target sites up to site 20, and we found no measurable off-target INDEL formation above the limit of detection (Supplementary Fig. 2b–e). AAV6-delivered donor templates for each linker antibody contain homology flanking the *CCR5* cut site and are driven by a previously defined B cell promoter, the EEK promoter (Fig. 2a), for strong expression in B lineage cells as the professional antibody secreting cell type[45].

Cord blood (CB) $CD34^+$ HSPCs were edited with each antibody construct individually through electroporation with RNP followed by immediate transduction with AAV6. We also edited cells with 10-1074 and Ibalizumab constructs in combination as proof of concept for simultaneous delivery of multiple antibodies. Knock-in analysis through in-out droplet digital PCR (ddPCR) determined that each antibody construct individually was incorporated in an average of 31% to 41% of alleles (Fig. 2b and Supplementary Fig. 3a). When used in combination, 10-1074 and Ibalizumab knock-in was detected in up to

https://doi.org/10.1038/s41467-025-58371-8

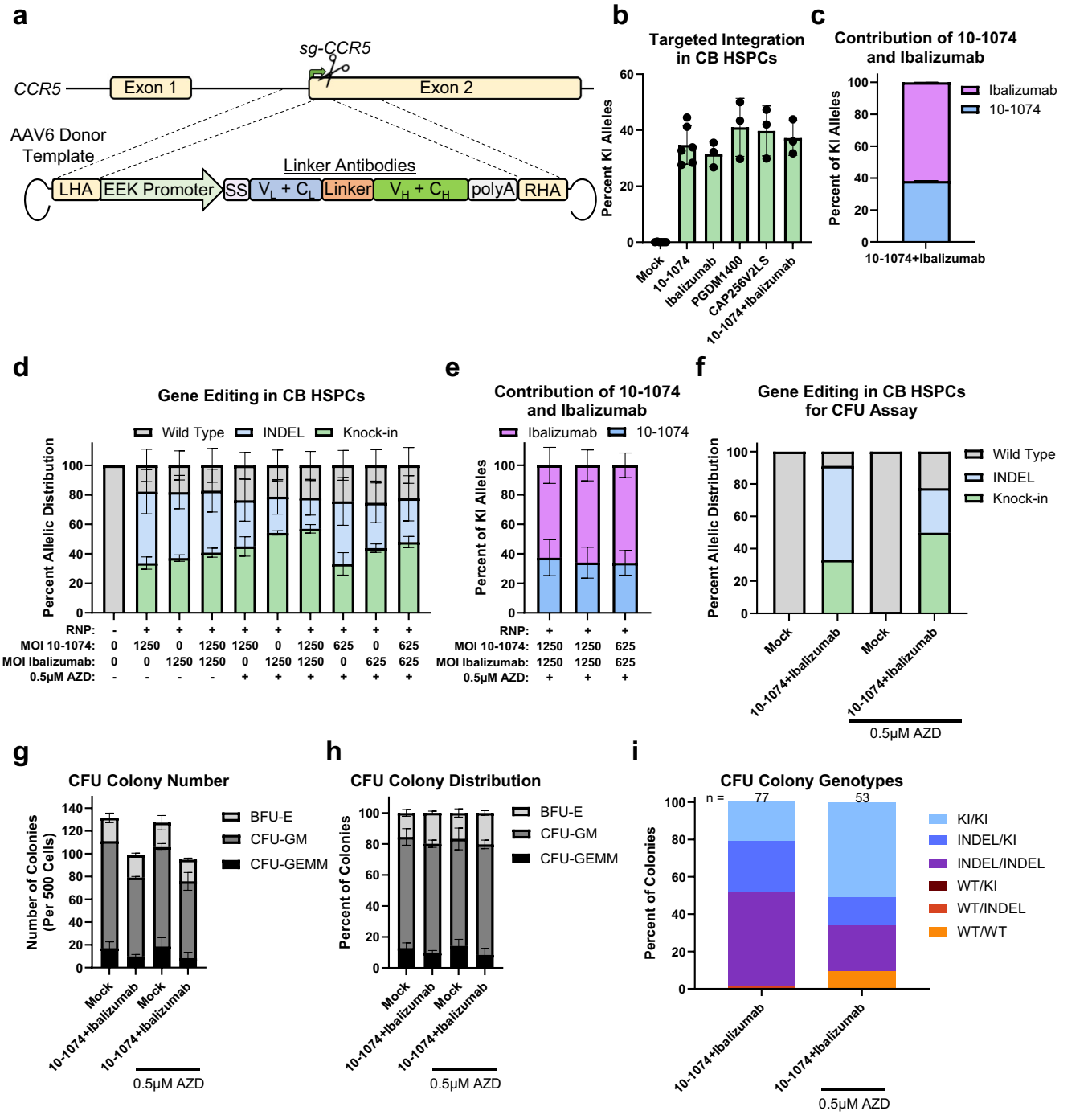

Fig. 2 | Efficient targeted integration of antibody expression cassettes at the *CCR5* locus in HSPCs. a Schematic of gene editing strategy to knock-in linker antibody expression cassettes at the *CCR5* locus. Created in BioRender. Feist, W. (2025) https://BioRender.com/l43f611. **b** Allelic integration frequency in CB CD34⁺ HSPCs targeted with AAV6 cassettes for linker antibodies as indicated. Each AAV6 was used at a multiplicity of infection (MOI) of 1250. Values represent independent biologic donors (n = 6 for mock and 10-1074 and n = 3 for Ibalizumab, PGDM1400, CAP256V2LS, and 10-1074+Ibalizumab). **c** Percent of (knock-in) KI alleles integrated with 10-1074 (blue) or Ibalizumab (purple) within the 10-1074+Ibalizumab targeted cells shown in **b** (n = 3). **d** Distribution frequency of WT (gray), INDEL (blue), and KI (green) alleles in CB CD34⁺ HSPCs targeted at *CCR5* with AAV6 MOI as indicated with or without 0.5 μM AZD7648 (AZD, n = 3). **e** Percent of knock-in alleles integrated with 10-1074 (blue) or Ibalizumab (purple) within the "10-1074+Ibalizumab" targeted cells shown in **d** (n = 3). **f** Distribution frequency of WT (gray), INDEL (blue), and KI (green) alleles in CB CD34⁺ HSPCs used for the CFU assay described in G, H, and I. Cell were targeted at *CCR5* with an AAV6 MOI of 625 for each construct with or without AZD7648 (n = 2). **g** Number of BFU-E (light gray), CFU-GM (dark gray), and CFU-GEMM (black) colonies formed per 500 cells plated (n = 2, with technical duplicates wells for each donor). **h** Relative frequency of BFU-E (light gray), CFU-GM (dark gray), and CFU-GEMM (black) colonies formed within the CFU assay (n = 2, with technical duplicate wells for each donor). **i** Frequency of genotypes from single-cell-derived colonies within the 10-1074+Ibalizumab targeted condition with or without AZD7648 (n represents the total number of colonies genotyped across both donors; KI/KI light blue, INDEL/KI dark blue, INDEL/INDEL purple, WT/KI maroon, WT/INDEL red, WT/WT orange). All replicates represent independent biological donors unless otherwise noted. All bars represent mean and error bars represent standard deviation (SD). Integration frequencies were measured by ddPCR, INDEL and wild-type frequencies were measured by ICE analysis. Source data are provided as a Source Data file.

44% of alleles. We designed a construct-specific ddPCR assay to determine the prevalence of each antibody within the bulk cell population and found slightly higher knock-in of the Ibalizumab cassette compared to 10-1074 (Fig. 2c and Supplementary Fig. 3a–d). While we focus on the use of 10-1074 and Ibalizumab together, further combinations can be made through editing with any two or three antibody cassettes simultaneously in CD34⁺ HSPCs (Supplementary Fig. 4).

Small molecule inhibition of NHEJ improves knock-in efficiency of antibody constructs

Inhibition of NHEJ by inhibiting DNA-PKcs with the small molecule AZD7648 has recently been shown to improve allelic knock-in frequency in RNP/AAV6 HDR-based editing[61]. Therefore, we tested the use of AZD7648 treatment with our constructs to increase editing frequency and reduce the multiplicity of infection (MOI) of AAV6 used for targeted knock-in. We found that AZD7648 treatment allowed us to reduce the AAV6 used by half while maintaining a high frequency of knock-in and *CCR5* KO resulting from either knock-in or INDEL formation (Fig. 2d). NHEJ inhibitor treatment did not impact the relative prevalence of 10-1074 and Ibalizumab in cells edited with both constructs (Fig. 2e).

To analyze the impact of AZD7648 treatment on differentiation capacity and cell health, we performed colony forming unit (CFU) assay analysis that measures myelo-erythroid differentiation potential in vitro. Two donors of CB CD34⁺ cells were treated with or without AZD7648 and received electroporation only (mock) or gene editing using a low MOI of both 10-1074 and Ibalizumab AAV6 together. As expected, we found that AZD7648 treatment increased knock-in frequency in the bulk cell population (Fig. 2f). AZD7648 treatment did not impact total colony formation or the distribution of colony formation between the three major sub-types, CFU-GEMM (colony forming unit-granulocyte, erythroid, macrophage, megakaryocyte), CFU-GM (colony forming unit-granulocyte and monocyte), and BFU-E (burst forming unit-erythroid) (Fig. 2g, h). Single colonies were genotyped to determine the impact of AZD7648 on mono-allelic and bi-allelic knock-in frequency, as well as INDEL formation. We found that AZD7648 treatment resulted in a 2.4-fold increase in the proportion of bi-allelic knock-in events across colony sub-types (21% to 51%) (Fig. 2i) and that just 9% of colonies maintained a wild-type (WT) allele following treatment with AZD7648. These results demonstrate that we can achieve efficient *CCR5* KO and knock-in of our antibody expression cassettes in CD34⁺ HSPCs, with further improved knock-in frequencies through the use of small molecule inhibition of NHEJ.

Engineered HSPCs engraft and reconstitute multiple hematopoietic lineages in immunodeficient mice

Genetically engineered HSPCs must maintain the ability to engraft and reconstitute the hematopoietic lineages in order to remain a viable therapeutic modality for long-term HIV-1 treatment. We therefore edited CB CD34⁺ cells with 10-1074, Ibalizumab, or both 10-1074 and Ibalizumab together (at higher AAV6 MOI and without AZD7648) and transplanted them in sub-lethally irradiated immunodeficient NSG mice (Fig. 3a). Prior to transplantation, we determined that each edited condition had similar frequencies of knock-in (33–38%) and *CCR5* KO INDEL formation (52-56%), with a slight prevalence of Ibalizumab knock-in in the combination edited cells (Fig. 3b, c). Engraftment, multilineage reconstitution, and editing frequencies of transplanted cells were measured at 16 weeks post-transplantation. Human chimerism was measured in bone marrow and spleen through flow cytometry analysis of human and mouse markers (Supplementary Fig. 5). Cells from each condition successfully engrafted in the bone marrow and showed migration to the spleen, a secondary lymphatic site, with similar human chimerism between each gene-edited condition (Fig. 3d, e). The observed decrease in total human engraftment due to RNP/AAV6-based editing was in line with previously published works[51,62–65]. Hematopoietic lineage distribution was consistent between conditions, with each editing condition producing similar frequencies of CD19⁺ B lineage cells and CD33⁺ myeloid lineage cells in both the bone marrow and spleen, indicating that our editing strategy does not introduce reconstitution bias (Fig. 3f, g). Knock-in alleles were present at the endpoint in both the bone marrow and spleen, though with a lower knock-in frequency than the bulk cells at the time of engraftment (Fig. 3h). This decrease in endpoint knock-in frequency is consistent with previous reports demonstrating an observed loss in engraftment potential of gene-targeted cells, perhaps due to toxicities associated with AAV6/RNP treatment and lower levels of knock-in in the long-term HSC population responsible for stable reconstitution[51,61–64,66,67]. Moreover, the decrease in endpoint knock-in frequency is consistent with previously published reports employing unrelated transgenes, indicating that the antibody cassettes are likely not introducing any further toxicity beyond that of the editing protocols alone[51,63,64]. Importantly, isolated CD19⁺ cells maintained knock-in alleles, indicating that integration of the antibody cassettes does not grossly inhibit early B cell formation, though, there was a reduction in knock-in compared with the bulk bone marrow (Fig. 3i). We note that this observed decrease in knock-in frequency is in line with previous reports and may indicate a general limitation in B cell reconstitution following editing and engraftment in this model[62,64,68]. *CCR5* KO alleles were also maintained in all conditions receiving RNP (Fig. 3j and Supplementary Fig. 6a). These analyses demonstrate that our engineered HSPCs engraft and reconstitute the hematopoietic lineages, providing promise for the development of an autologous transplant therapy. However, the relatively low frequency of integrated alleles in the cells at the engraftment endpoint warranted further optimization. The results shown in Fig. 2 demonstrated that one approach to optimization is to incorporate DNA-PKcs inhibition while lowering the MOI of AAV6.

High-efficiency editing with low AAV6 MOI in CD34⁺ HSPCs results in maintenance of integrated alleles following engraftment in vivo

Achieving a high frequency of integrated antibody cassettes in engrafted cells will be important for future studies determining the minimum editing threshold needed to achieve clinically relevant concentrations of each antibody. We therefore sought to modify our editing protocols to improve maintenance of edited alleles following engraftment. To this end, we employed AZD7648 treatment to augment our knock-in protocol prior to transplantation. AZD7648 has been shown to improve knock-in frequencies in both bulk CD34⁺ and long-term HSPCs[61]. Additionally, the use of AZD7648 allowed us to employ reduced AAV6 doses while maintaining knock-in frequencies (Fig. 2d, f) to potentially improve cell health and engraftment of edited cells, as reducing AAV6 is known to reduce the p53 response in HSPCs[61,69]. Two donors of CB CD34⁺ cells were edited with AZD7648 and a low AAV6 MOI for knock-in of both 10-1074 and Ibalizumab and transplanted into non-conditioned NBSGW immunodeficient mice. Input cells carried a knock-in frequency averaging 50% with efficient knock-in of both 10-1074 and Ibalizumab constructs (Fig. 4a, b). Human chimerism and lineage formation were analyzed in the bone marrow at 12 weeks post-transplantation. Gene-edited cells engrafted at a lower frequency than mock edited cells, though this decrease is in line with those seen in the literature (Fig. 4c)[51,62–65]. As seen in previous reports when human chimerism is low, gene-edited HSPCs showed a myeloid bias in reconstitution within the bone marrow (Fig. 4d)[51,63]. Importantly, we found the allelic knock-in frequency in the endpoint engrafted cells to remain above 50% (52–80%) in all but one mouse (11%) (Fig. 4e). Knock-in

https://doi.org/10.1038/s41467-025-58371-8

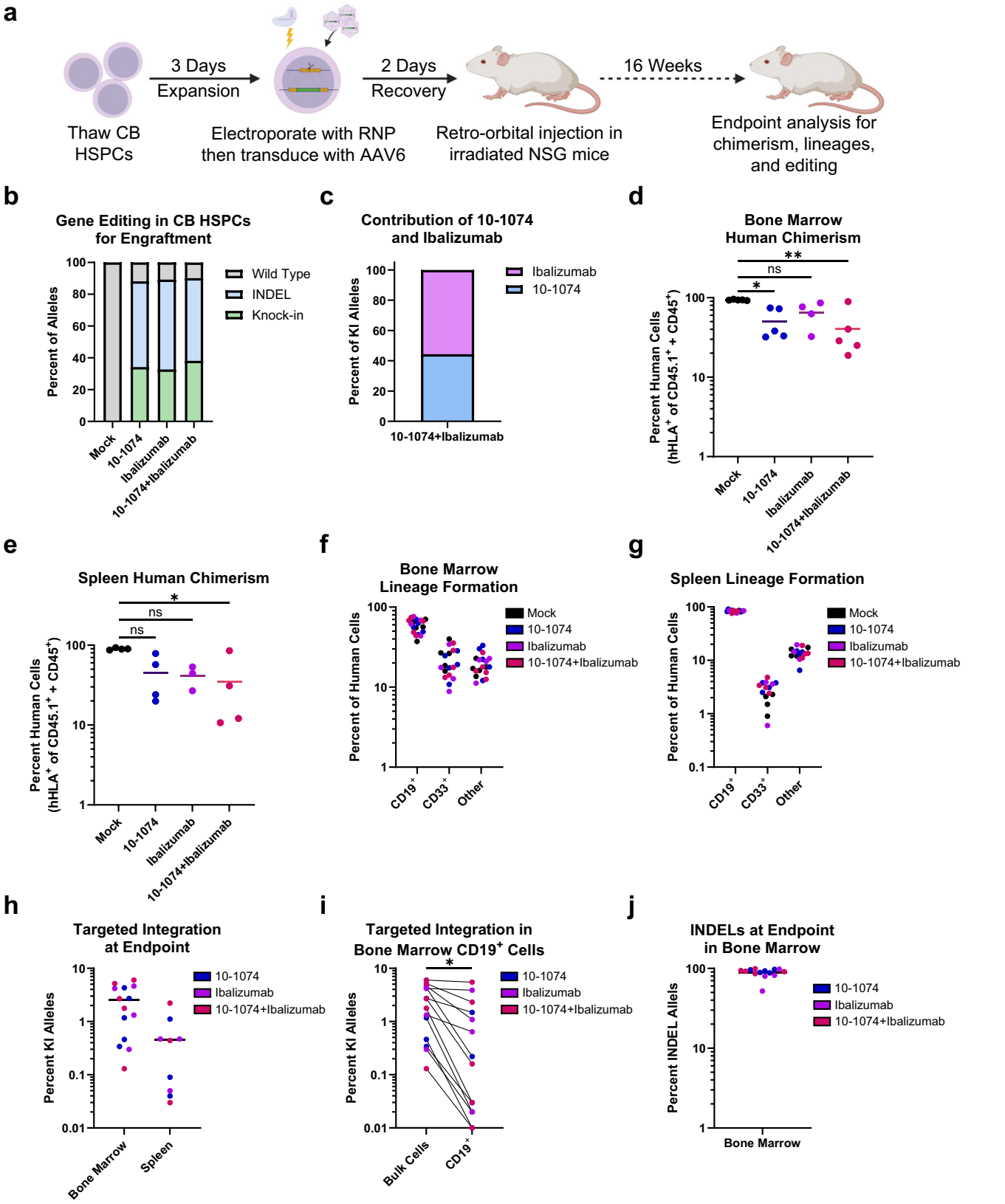

frequency was also maintained in the CD19$^+$ B cell lineage population within the bone marrow, with consistent frequencies of both 10-1074 and Ibalizumab constructs, further demonstrating that the knock-in of our constructs does not impact early B cell formation (Fig. 4e and Supplementary Fig. 6b, c). Finally, *CCR5* KO INDELs were also maintained in non-integrated alleles (Fig. 4f). While direct comparisons between cells treated with and without AZD7648 and low dose AAV6 are still needed, these results introduce an editing protocol that could be used to maintain the frequency of edited alleles within the long-term engrafted cell population. Such an improvement provides a favorable editing profile for introducing both *CCR5* KO and long-term expression from our therapeutic antibody cassettes.

While we were able to achieve efficient engraftment of gene-edited cells, this model limits our ability to effectively analyze the in vivo

https://doi.org/10.1038/s41467-025-58371-8

Fig. 3 | Antibody edited HSPCs maintain engraftment capacity and multi-lineage reconstitution in vivo. a Diagram for editing and engraftment of CB CD34⁺ HSPCs in NSG mice. Created in BioRender. Feist, W. (2025) https://BioRender.com/l43f611. **b** Distribution frequency of WT (gray), INDEL (blue), and KI (green) alleles in CB CD34⁺ HSPCs prior to transplantation. Cells were targeted with an AAV6 MOI of 1250 for each construct (n = 1 pooled sample from 5 donors). **c** Percent of KI alleles integrated with 10-1074 (blue) or Ibalizumab (purple) within the 10-1074+Ibalizumab targeted cells in panel **b** (n = 1). **d** Percent human chimerism in the bone marrow at endpoint (n = 5 mice for mock, 10-1074, and 10-1074+Ibalizumab, n = 4 for Ibalizumab). One-way ANOVA Kruskal-Wallis test plus Dunn's multiple comparisons test (ns, not significant, P = 0.3287; *P = 0.0496; **P = 0.0082). **e** Percent human chimerism in the spleen at endpoint (n = 4 for mock, 10-1074, and 10-1074+Ibalizumab, n = 3 for Ibalizumab). One-way ANOVA Kruskal-Wallis test plus Dunn's multiple comparisons test (ns, not significant, P = 0.0806 for Mock/10-1074, P = 0.1363 for Mock/Ibalizumab; *P = 0.0216). **f** Percent of human cells in the bone marrow (n are the same as in **d**) or **g** spleen (n are the same as in **e**) that are CD19⁺, CD33⁺, or within other lineages in mice engrafted with mock (black) or gene edited HSPCs (10-1074, blue; Ibalizumab, purple; 10-1074+Ibalizumab, red). **h** Percent of KI human alleles from the bone marrow or spleen (n are the same as in (**d**, **e**), respectively). **i** Percent of KI human alleles from the bulk bone marrow (shown in panel **h**) or from bone marrow CD19⁺ cells (n are the same as in **d**). Lines connect measurements from the same mice. Two-tailed Mann–Whitney test (*P = 0.0135). **j** Percent of human alleles with an INDEL at *CCR5* (n are the same as in **d**). This analysis only includes alleles without KI. All bars represent mean. Integration frequencies were measured by ddPCR, INDEL and wild-type frequencies were measured by ICE analysis. Source data are provided as a Source Data file.

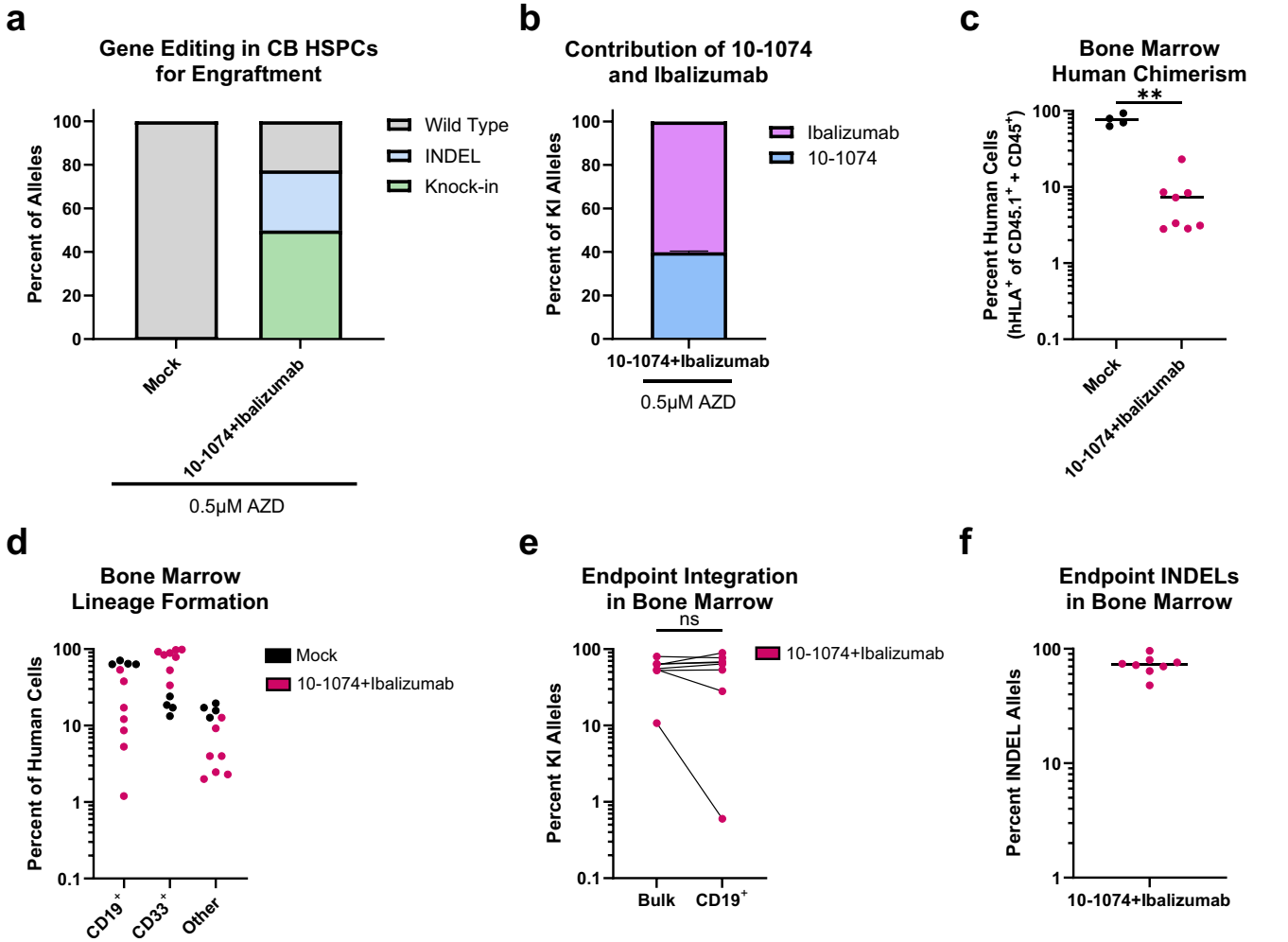

Fig. 4 | HSPCs with high frequency knock-in maintain edited alleles following engraftment in vivo. a Distribution frequency of WT (gray), INDEL (blue), and KI (green) alleles in CB CD34⁺ HSPCs prior to transplantation in NBSGW mice. Cells were targeted at *CCR5* with an AAV6 MOI of 625 for each linker antibody construct and treated with 0.5 μM AZD7648 (n = 2 independent biologic donors; data also shown in Fig. 2f). **b** Percent of KI alleles integrated with 10-1074 (blue) or Ibalizumab (purple) within the 10-1074+Ibalizumab targeted cells treated with 0.5 μM AZD7648 and shown in panel a (n = 2). **c** Percent human cell chimerism in the bone marrow 12 weeks post-transplantation with cells shown in panel **a** (treated with 0.5 μM AZD7648 and targeted as indicated). Two-tailed Mann–Whitney test (**P = 0.0040, n = 4 mice for mock and n = 8 mice for 10-1074+Ibalizumab). **d** Percent of human cells in the bone marrow that are CD19⁺ (B cell lineage), CD33⁺ (myeloid cell lineage), or within other lineages in mice engrafted with mock (black) or gene edited (red) HSPCs (n are the same as in **c**). **e** Percent of human alleles with knock-in from the bulk bone marrow or in positively selected bone marrow CD19⁺ cells. Knock-in frequency was measured by ddPCR. Lines connect measurements from the same mice (n are the same as in **c**). Two-tailed Mann–Whitney test (ns, not significant, P = 0.7178). **f** Percent of human alleles from the bone marrow with an INDEL at *CCR5* (n are the same as in **c**). This analysis only includes alleles without KI. All bars represent mean and all error bars represent SD. Integration frequencies were measured by ddPCR, INDEL and wild-type frequencies were measured by ICE analysis. Source data are provided as a Source Data file.

capacity of our system to secrete antibodies. It is well known that human HSPCs transplanted into NSG background mice do not efficiently mature into highly differentiated human B cells[70,71]. This is highlighted by our results and others showing that even mice engrafted with high human chimerism do not produce relevant levels of human IgG (Supplementary Fig. 7)[71–73]. While both humans and immunocompetent mice are expected to produce over 6 mg/mL of IgG, we observed less than 300 ng/mL (>4 logs lower) in the serum of humanized mice in all but one mouse (4.5 μg/

mL, 3 logs lower). Therefore, other models beyond xenotransplantation in immunodeficient mice are needed to assess the functional secretion of antibodies within our system.

Engineered human B cells secrete functional levels of each HIV-1 inhibiting antibody

Due to limitations in the humanized mouse model, we were unable to directly demonstrate if B cells derived from engineered HSPCs produce therapeutically relevant concentrations of linker antibodies in vivo. To bridge this gap, we sought to directly edit adult peripheral blood $CD19^+$ B cells at the *CCR5* locus with the same RNP/AAV6 guide RNA and antibody constructs used in HSPCs. We first confirmed the function of the EEK promoter in adult B cells through knock-in of constructs driving GFP expression through either the EEK promoter (EEK-GFP) or the strong ubiquitous ubiquitin C (UBC) promoter (UBC-GFP) (Supplementary Fig. 8a, b). The EEK-GFP construct was integrated within the *CCR5* locus at the same site as each antibody expression construct. Of note, UBC-GFP was a previously published construct that integrates 206 bases downstream within the *CCR5* coding region, somewhat limiting its use for direct comparison with EEK-GFP[51,61]. Flow cytometry analysis for median fluorescent intensity (MFI) of GFP^+ cells was higher when driven by the EEK promoter, indicating its strong activity in B cells (Supplementary Fig. 8c). Next, we edited B cells with each linker antibody construct individually or with combinations of the 10-1074 and Ibalizumab constructs together or 10-1074 and CAP256V2LS constructs together. As with $CD34^+$ HSPCs, we achieved highly efficient knock-in into the *CCR5* locus at frequencies up to 43% of alleles (Fig. 5a). Additionally, the knock-in of an exogenous antibody cassette did not obviously impact any B cell subset within the in vitro culture system (Supplementary Fig. 9)[74].

We next demonstrated that the knock-in of the EEK-driven linker antibody constructs resulted in the secretion of functional antibodies. B cells were edited, allowed to recover for six days, and then plated at a density of 1 million cells per mL of media for five days. Culture supernatant was collected, and antigen-specific ELISA analysis was used to confirm the presence of each antibody (Fig. 5b). As expected within this system, both HIV-inhibiting antibodies from the *CCR5* locus and endogenous antibodies from the *IgH* locus were produced by the bulk engineered B cells (Supplementary Fig. 10). We observed that B cells edited with an average knock-in frequency of 33% (donors 1, 2 and 3 from Fig. 5a) produced linker 10-1074 at an approximate ratio of 1:30 relative to endogenous IgG. This result indicates that, on a per cell basis, the EEK promoter expresses with approximately 1/10th the strength of the endogenous *IgH* promoter.

With individual B lineage cells potentially expressing endogenous IgG alongside the exogenous HIV-inhibiting antibodies, we sought to explore how co-expression of traditional and linker antibodies would impact antibody formation. Where inclusion of the peptide linker is intended to prevent the mispairing of a linker light or heavy chain directly with an endogenous heavy or light chain, respectively, it is possible that a linker light and heavy chain pair could couple with an endogenous light and heavy chain pair via the IgG constant region, forming a bi-specific product we refer to as a "mixed-chain" antibody. We sought to model the co-expression of linker and traditional IgGs by simultaneously expressing linker 10-1074 and an unrelated SARS-CoV-2 specific IgG1 (S2-4) in the Expi293F cell line[75]. We employed mass spectrometry analysis to measure the formation of traditional antibodies (expected 149 kDa), linker antibodies (expected 159 kDa), and mixed-chain antibodies (expected 154 kDa) (Supplementary Fig. 11a) and found that mixed-chain antibodies were indeed formed alongside traditional and linker antibodies. We then performed mass spectrometry analysis on total IgG isolated from B cells engineered for expression of the linker antibody cassettes. We detected secretion of both endogenous IgGs (~146–151 kDa) and mixed-chain linker-endogenous antibodies (approximately 154 kDa) without detecting any larger mispaired aggregated species that could result from mispairing of linker light or heavy chains with endogenous heavy or light chains, respectively (Supplementary Fig. 11b). The presence of mixed-chain antibodies indicates that B cells with exogenous antibody knock-in at *CCR5* do simultaneously express linker and endogenous antibodies. This finding represents an important indication that B cells can maintain their natural function while expressing exogenous antibodies.

We next sought to determine if the mixed linker-endogenous antibodies maintained their inhibitory function when expressed from B cells. Serial dilutions of cell culture supernatant were tested for neutralization potency in the TZM-bl infection assay against either TRO11 or CNE55 HIV-1 pseudoviruses for which we empirically determined the expected IC_{50} for each antibody in Fig. 1c (Fig. 5c). Supernatant from B cells edited with 10-1074 and Ibalizumab cassettes individually inhibited infection, with near complete inhibition at a 1:2 media dilution (Fig. 5d and Supplementary Fig. 12d). As expected from the known IC_{50} values, PGDM1400 supernatant showed a reduced inhibition capacity and CAP256V2LS supernatant did not inhibit infection with TRO11. When tested against CNE55, we found that supernatant from B cells expressing 10-1074 did not inhibit infection, while supernatant from B cells expressing Ibalizumab, PGDM1400, and CAP256V2LS each effectively inhibited infection corresponding with the known IC_{50} of each antibody (Fig. 5e and Supplementary Fig. 12d). We then sought to mirror combination antibody therapies through engineering B cells for the simultaneous expression of two antibodies together (Fig. 5d, e and Supplementary Fig. 12b, c). Where 10-1074 alone is ineffective against CNE55 and CAP256V2LS alone is ineffective against TRO11, culture supernatant from B cells expressing both antibodies together effectively inhibits both pseudoviruses, highlighting the importance of simultaneously employing multiple antibodies to overcome deficiencies of any single antibody (Fig. 5d, e). These results demonstrate that B cells carrying linker antibody expression cassettes are capable of effectively secreting inhibitory concentrations of antibodies individually and in combination, and that these linker antibodies retain function when expressed directly from B cells. Additionally, the successful expression of two antibodies together further highlights the significance of a multi-epitope targeting strategy for efficacy against diverse HIV-1 strains.

Discussion

The transplantation of HSPCs that generate HIV-resistant progeny represents a promising strategy to achieve a functional cure for HIV-1. However, the currently established method for allogeneic transplantation of *CCR5* KO HSPCs is limited due to the rarity of available donor cells, the risk for GvHD, and a lack of efficacy against X4-tropic virus. Transplantation of genetically engineered autologous HSPCs is a treatment modality with the potential to address these limitations. Modifying a patient's own cells removes the need for identifying a matched donor and circumvents the risks specific to allogeneic transplantation. Additionally, precise genetic engineering can allow for the delivery of multi-factored resistance to R5-tropic and X4-tropic HIV-1. To this end, we have established a highly efficient genome editing strategy to combine the known benefits of *CCR5* KO with antibody therapy in a manner applicable towards autologous HSPC transplantation.

Here we demonstrate the simultaneous knockout of *CCR5* and knock-in of antibody expression cassettes in human HSPCs for secretion of HIV-1 inhibiting antibodies in B cell progeny of edited cells. Following transplantation, genetically engineered HSPCs have the potential to persist for a patient's lifetime and provide a long-term source of therapeutic antibody secreting B cells. Recent trials investigating direct injection of bNAbs for HIV-1 suppression show that repeated dosing is required to maintain efficacy, as viral titers rebound once the serum concentrations drop below a therapeutic threshold[18,19]. Additionally, AAV and B cell-mediated antibody delivery platforms rely

https://doi.org/10.1038/s41467-025-58371-8

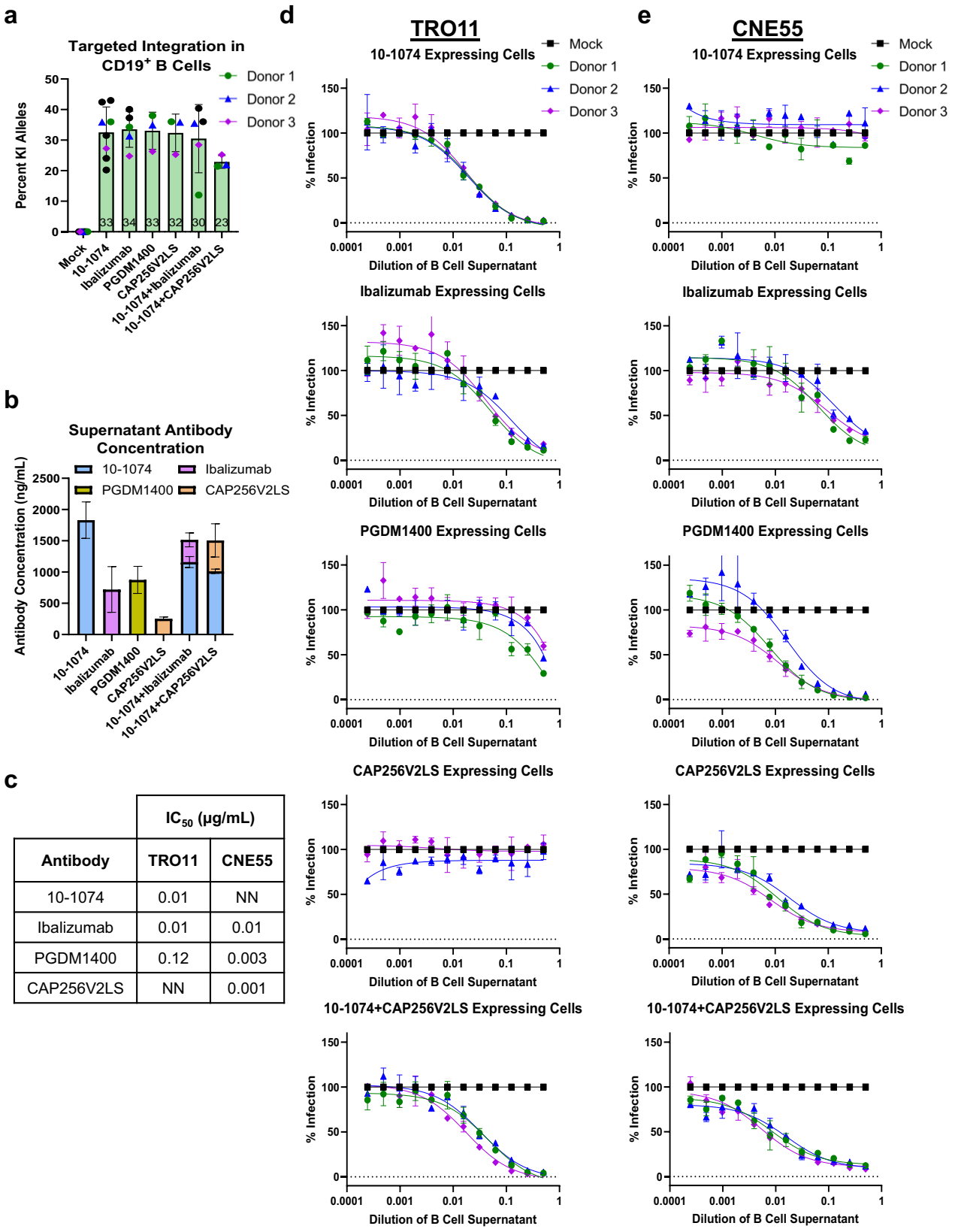

Antibody	IC_{50} (μg/mL) TRO11	CNE55
10-1074	0.01	NN
Ibalizumab	0.01	0.01
PGDM1400	0.12	0.003
CAP256V2LS	NN	0.001

on somatic cells and are unlikely to rival the longevity of HSCT. Therefore, the engraftment of genetically engineered HSPCs represents one of the most promising methods for a one-time therapy to combat HIV-1. To this end, we show that RNP/AAV6 editing of HSPCs delivers a favorable profile of modified alleles, achieving a knock-in frequency of up to 50% of alleles and KO frequency of up to 90% of alleles at *CCR5* (Fig. 2). Importantly, engineered HSPCs engraft and reconstitute the hematopoietic lineages in immunodeficient mice (Fig. 3), though with reduced engraftment capacity compared to mock edited cells. We find that an altered protocol employing small molecule inhibition of NHEJ and reduced AAV6 MOI may be used to address the decrease in knock-in alleles normally seen following engraftment

Fig. 5 | Antibody engineered B cells secrete functional linker antibodies. **a** Allelic integration frequency in adult peripheral blood CD19⁺ B cells targeted with AAV6 cassettes for linker antibodies as indicated. Each AAV6 was used at an MOI of 25,000 and integration frequency was measured with ddPCR (dots represent independent biologic donors, n = 8 for mock and 10-1074, n = 5 for Ibalizumab and 10-1074+Ibalizumab, n = 3 for PGDM1400 and CAP256V2LS). Donor 1 (green circle), Donor 2 (blue triangle), and Donor 3 (purple diamond) are specifically noted for their continued use in (**b**, **d**, **e**). Bars represent mean and error bars represent SD. **b** Concentration of each antibody (10-1074, blue; Ibalizumab, purple; PGDM1400, gold; CAP256V2LS, orange) as determined by antigen specific ELISA from B cell supernatant from cells targeted with AAV6 cassettes as indicated (n = 3 biological donors comprised of Donor 1, Donor 2, and Donor 3 from **a**). Six days post-editing, B cells were plated at 1×10^6 cells per mL and supernatant was collected after 5 days. Bars represent mean and error bars represent SD. **c** Measured IC_{50} for each antibody against TRO11 or CNE55 pseudoviruses as determined by TZM-bl assay in Fig. 1c (NN, not-neutralizing). **d** Inhibition of infection with TRO11 or **e** CNE55 HIV-1 pseudovirus by culture supernatant from B cells engineered to express linker antibodies as indicated, as determined by TZM-bl assay. Percent infection for each dose of supernatant from gene targeted B cells is normalized to infection at each dose of supernatant from mock B cells from the same donor (n = 3 biological donors; Donor 1 (green circle), Donor 2 (blue triangle), and Donor 3 (purple diamond) from **a**). Data points and error bars represent mean with range of technical duplicate infections. Source data are provided as a Source Data file.

(Fig. 4). The development of this system for highly efficient *CCR5* KO and knock-in of antibody expression cassettes is a favorable first step towards developing an autologous transplantation therapy.

Recently, the transplantation of gene edited autologous HSPCs has displayed clinical success with the approval of Casgevy for the treatment of sickle cell disease and beta-thalassemia[50,76]. Casgevy uses RNP editing for INDEL generation in HSPCs, acting as a proof of concept for RNP-edited HSCT. Now, efforts are underway to expand the therapeutic potential of CRISPR-Cas9 editing to include knock-in of large therapeutic cassettes using AAV6/RNP mediated editing. However, it is regularly shown that AAV6 treatment negatively impacts HSPCs, as demonstrated through reduced colony formation in CFU assays and decreased chimerism following xenotransplantation[77]. We and others are exploring methods to alleviate toxicity associated with AAV6 in HSPCs to improve the long-term engraftment of engineered cells. For one, the use of small molecule NHEJ inhibitors allows for reduced doses of AAV6 and RNP to achieve the same editing frequencies, potentially decreasing toxicity through a reduction in p53 activation[61,69,78]. Additionally, inhibition of the cell's DNA damage response through transient inhibition of 53BP1 with peptides or siRNA has been shown to reduce toxicity in HSPCs[78,79]. Finally, it has been demonstrated that simply increasing the number of transplanted cells can compensate for AAV6 associated toxicity in xenograft mouse models[64]. While more work is needed to refine optimal editing conditions and improve engraftment of AAV6/RNP-edited HSPCs, the data presented here represent an important proof of concept study for the efficacy of a long-term antibody delivery platform for treatment of HIV and other diseases treatable by recombinant antibody delivery.

Engraftment in immunodeficient mice is the gold-standard for functional analysis of genetically engineered human HSPCs, however, the model fails to recapitulate normal B cell development and maturation. While our engineered HSPCs do engraft and maintain edited alleles in CD19⁺ progeny, we are not able to assess functional antibody expression due to a lack of mature antibody secreting B cells in vivo. To address our system's ability to drive therapeutic antibody expression, we edited adult peripheral blood B cells with the same constructs used in HSPCs. These modified B cells were capable of secreting inhibiting levels of each tested antibody into the culture supernatant (Fig. 5). It is well known that multiple antibodies should be employed simultaneously to combat viral diversity and escape. We therefore designed our system for use with multiple antibodies concurrently and show that linker 10-1074 and linker CAP256V2LS could be expressed together from one bulk population of B cells (Fig. 5). The modular design of our cassettes permits antibodies to be readily switched out, allowing for optimization of antibody pairings and potential customization based on the viral diversity of various patient populations across regions.

Because B lineage cells are the professional antibody-producing cells of the hematopoietic system, we believe that expression from B cell progeny is a favorable strategy for sustained delivery of engineered antibodies. By knocking into the *CCR5* locus, the presented engineering strategy does not disrupt the IgH-locus. Therefore, the antibody expression cassettes should act as passengers to normal B cell function and be capable of persisting across B cell sub-types. We expect that hematopoietic reconstitution with engineered HSCs will produce a steady supply of engineered B lineage cells, with therapeutic plasma cells arising from normal participation in the humoral immune response alongside unmodified B cell progeny. Furthermore, we envision that standardized vaccinations currently used to limit infection following HSCT will help to establish an early population of engineered plasma cells[80]. Over time, as transplanted HSCs continue to reconstitute the hematopoietic system, the fraction of B lineage and plasma cells carrying our antibody expression cassettes will likely mirror that of the engrafted HSCs. This will ideally allow for our antibodies to reach a steady-state concentration in the bloodstream, providing an advantage over traditional antibody injection therapies that have peaks and troughs with each administration. Moreover, the antibody production data presented in this study allows us to roughly calculate the potential output of engineered B cells. We found that engineered B cells produced linker 10-1074 at an approximate ratio of 1:10 relative to endogenous IgG. Given that human serum contains 8000 to 18,000 μg/mL IgG, we could see 8–18 μg/mL of therapeutic antibody for every 1% of knock-in alleles. Therefore, engraftment of cells with 30% knock-in could potentially allow for 240–540 μg/mL of HIV-inhibiting antibodies. While further in vivo modeling is needed to determine the actual production capacity, this rough calculation shows the potential for delivery of therapeutically relevant antibody concentrations within our system. Additionally, given the tolerance for large bolus injections seen with these HIV-inhibiting antibodies, there is a broad therapeutic window where we do not expect overproduction from engineered cells to be a concern. Moving forward, future studies will certainly be required to determine the frequency of knock-in in HSPCs needed to achieve clinically relevant secretion of each therapeutic antibody while limiting the potential for overproduction.

Expression of the therapeutic antibodies from B cells directly may further benefit from the inclusion of natural post-translational modifications that are not incorporated when expressed from other cell types[81]. Carrying these modifications may decrease immune recognition of HIV-1 inhibiting antibodies and reduce the potential for anti-drug antibody formation, an issue encountered by both vectored immunoprophylaxis and direct injection trials[24,27,82,83]. Additionally, endogenous glycosylation and sialylation have the potential to improve F_C-mediated clearance of HIV-1 infected cells[84,85]. Moving forward, it will be important to investigate the impact of post-translational modifications on antibodies expressed from B cells.

Given the limitations in B cell maturation, formation of circulating B cells, and antibody secretion within humanized mice, further in vitro models and non-human primate models will be important in establishing pre-clinical safety and efficacy. This study presents inhibition of pseudoviruses with supernatant from engineered B cells as a proof of concept. However, further pre-clinical studies should investigate efficacy against a range of primary isolates as a more stringent functional test for the B cell secreted linker antibodies. Additionally, future works may seek to engineer our system for editing in rhesus macaque HSCs,

which would efficiently differentiate to antibody expressing B lineage cells following engraftment in vivo. This would allow for valuable analysis of B cell maturation and characterization of editing frequencies in circulating B cells and plasma cells. Another important benefit of this model is the ability to challenge with simian-human immunodeficiency virus (SHIV), allowing for studies into the therapeutic window for each antibody combination and characterization of the impact of mixed-chain antibody formation on safety and efficacy in vivo.

While the described system is designed with a B cell specific promoter for consistent antibody expression linked to normal humoral responses, future works should investigate the use of inducible systems to provide precise control of antibody levels. While more development is needed to design a B cell specific inducible promoter, other inducible promoters systems could be considered for small molecule control of antibody expression from hematopoietic cells[86]. Alternatively, advancements in degron systems may allow for use of B cell specific promoters with each antibody fused with a degron domain[87–89]. Though, careful analysis of antibody-degron fused proteins will be needed to ensure function and characterize immune recognition of degron peptides. Additionally, safety switches, such as inducible caspase 9, could be included to allow for efficient clearing of engineered cells to modulate the cell therapy[90,91]. These inducible systems may be useful in maintaining transgene antibody levels within a therapeutic window that prevents escape mutant formation while minimizing potential for side effects from overexpression.

Overall, this work serves as a platform strategy for the lifetime secretion of desired therapeutic antibodies. Beyond its usefulness for HIV-1 resistance, knock-in into the *CCR5* safe harbor site allows for broad applications across chronic diseases. Future works will test alternate antibodies for use within our system as a alternative delivery modality for current treatment regimens that require long-term dosing of monoclonal antibodies.

Methods

Ethics statement

Umbilical cord blood-derived HSPCs were obtained from Binns Program for Cord Blood Research with approval from the Stanford Institutional Review Board Committee under protocol 33813. All donors provided informed consent, and participant information was deidentified. All research involving mice was completed at Stanford University and complied with all relevant ethical regulations. All animal procedures and experiments were reviewed and approved by the Stanford University Administrative Panel on Laboratory Animal Care (Protocol #25065).

rAAV6 vector design, production, and purification

The sequence of each antibody construct was cloned from a gblock Gene Fragment (Integrated DNA Technologies, IDT, San Jose, CA, USA). Restriction enzyme digest or Gibson Assembly (New England Biolabs, Ipswich, MA, USA) was used to clone each antibody sequence plus 400 base pair (bp) homology arms on each side of the construct into an adeno-associated virus, serotype 6 (AAV6) vector plasmid derived from the pAAV-MCS plasmid (Agilent Technologies, Santa Clara, CA, USA). Experiments were performed with rAAV6 vectors produced and purified by SignaGen Laboratories (Frederick, MD, USA) and Packgene Biotech (Houston, TX, USA). All viral titers were determined using droplet digital PCR (ddPCR; Bio-Rad) to measure the absolute number of vector genomes using a previously reported primer and probe set targeting the inverted terminal repeats[92]. The primers and probe are as follows:

Forward Primer (FP): 5′-GGAACCCCTAGTGATGGAGTT-3′
Reverse Primer (RP): 5′-CGGCCTCAGTGAGCGA-3′
Probe: 5′-6-FAM/CACTCCCTC/ZEN/TCTGCGCGCTCG/3IABkFQ/-3′

CD34$^+$ HSPC isolation and culture

Human CD34$^+$ HSPCs were isolated from cord blood by the Stanford Binns Program for Cord Blood Research and cultured as previously described[93]. Samples were obtained with approval from the Stanford Institutional Review Board Committee under protocol 33813. The samples were obtained deidentified and no demographics were collected. Sex and/or gender were not considered in the study design of any experiment using these samples. Briefly, isolated mononuclear cells were positively selected for CD34 using the CD34+ Microbead Kit Ultrapure (Miltenyi Biotec, San Diego, CA, USA, cat.: 130-100-453). Cells were cultured at 1.5×10^5–2.5×10^5 cells/mL in CellGenix® GMP Stem Cell Growth Medium (SCGM, CellGenix, Freiburg, Germany, cat.: 20802-0500) supplemented with a human cytokine (PeproTech, Rocky Hill, NJ, USA) cocktail: stem cell factor (100 ng/mL), thrombopoietin (100 ng/mL), Fms-like tyrosine kinase 3 ligand (100 ng/mL), interleukin 6 (100 ng/mL), streptomycin (20 mg/mL), and penicillin (20 U/mL), and 35 nM of UM171 (APExBIO, Houston, TX, USA, cat.: A89505). Cells were cultured in a 37 °C hypoxic incubator with 5% CO_2 and 5% O_2. Cells were cultured for 3 days prior to editing.

Genome editing of HSPCs

HPLC-purified synthetic chemically modified sgRNAs were purchased from TriLink Biotechnologies (San Diego, CA, USA). Chemical modifications were comprised of 2′-O-methyl-3′-phosphorothioate at the three terminal nucleotides of the 5′ end and the second, third, and fourth bases from the 3′ end as described previously[94]. The target sequence for the sgRNA are as follows: sg-*CCR5*, 5′-ATGCACAGGGTGGAACAAGA-3′; sg-*CCR5-#2*, 5′-GCAGCATAGTGAGCCCAGAA-3′. HiFi Cas9 protein was purchased from IDT (cat.: 1081061) or Aldevron (Fargo, ND, USA, cat:. 9214). RNPs were complexed at a Cas9:sgRNA molar ratio of 1:2.5 at room temperature for 15–30 min. 2.5×10^5–1×10^6 CD34$^+$ cells were resuspended in P3 buffer (Lonza, Basel, Switzerland, cat.: V4XP-3032) with complexed RNPs and electroporated using the Lonza 4D Nucleofector and 4D-Nucleofector X Unit (program DZ-100). Electroporated cells were then plated at 2.5×10^5 cells/mL in the previously described cytokine-supplemented media. Immediately following electroporation, AAV6 was dispensed onto cells at 0.625×10^3–2.5×10^3 vector genomes/cell as noted in figure legends. For some editing experiments, in addition to the steps described above, cells were incubated with 0.5 μM of DNA-PKcs inhibitor, AZD7648 (Selleck Chemicals, Houston, TX, cat.: S8843) for 24 h, as previously described[61].

B cell isolation, culture, and genome editing

Leukoreduction system (LRS) chambers were obtained from the Stanford Blood Center and primary human B cells were isolated by negative selection using the human B Cell Isolation Kit II (Miltenyi Biotec, cat: 130-091-151). The samples were obtained deidentified and no demographics were collected. Sex and/or gender were not considered in the study design of any experiment using these samples. Cells were cultured in Iscove's modified Dulbecco's medium (IMDM) (Thermo Fisher Scientific, Waltham, MA, USA cat.: 12440053) supplemented with 10% bovine growth serum (Cytiva, Marlborough, MA, USA, cat.: SH30541.03HI), 1% penicillin-streptomycin (Cytiva, cat.: SV30010), 55 μM of 2-mercaptoethanol (Sigma-Aldrich, St. Louis, MO, USA, cat.: M3148), 50 ng/mL of IL-2 (Peprotech, cat.: 200-02), 50 ng/mL of IL-10 (Peprotech, cat.: 200-10), 10 ng/mL of IL-15 (Peprotech, cat.: 200-15), 100 ng/mL of recombinant human MEGACD40L (Enzo Life Sciences, Farmingdale, NY, USA, cat.: ALX-522-110-C010), and 1 μg/mL of CpG oligonucleotide 2006 (Invivogen, San Diego, CA, USA cat.: tlrl-2006-1) at a density of 1×10^6 cells/mL, as described previously[28]. B cells were cultured at 37 °C, 5% CO_2, and ambient oxygen levels. Genome editing was performed as described above for HSPCs with the following modifications. B cells were edited 3–5 days after isolation or thawing using the Lonza Nucleofector 4D (program EO-117) using

1×10^6 cells per well of a 16-well Nucleocuvette Strip (Lonza). Immediately following nucleofection, cells were incubated with AAV6 donor vector (2.5×10^4 vector genomes/cell) in 100 μl of basal IMDM in a 96 well plate for 3–4 hours and then replated at 1×10^6 cells/mL in complete B cell activation media[95].

Measurement of knock-in alleles by ddPCR

Cells were harvested 2–3 days post-electroporation and genomic DNA (gDNA) was harvested using QuickExtract DNA extraction solution (Biosearch Technologies, Hoddesdon, UK, cat.: QE09050). To quantify knock-in alleles via ddPCR, we employed *CCR5* specific in-out PCR primers and a probe corresponding to the expected knock-in event (1:3.6 primer to probe ratio)[63]. We also used an established genomic DNA reference (REF) at the *CCRL2* locus[63]. The ddPCR reaction was prepared and underwent droplet generation following the manufacturer's instructions with a Bio-Rad QX200 ddPCR machine (Bio-Rad, Hercules, CA, USA). Thermocycler settings were as follows: 95 °C (10 min, 1 °C/s ramp), 94 °C (30 s, 1 °C/s ramp), 60 °C (30 s, 1 °C/s ramp), 72 °C (2 min, 1 °C/s ramp), return to step 2 for 50 cycles, and 98 °C (10 min, 1 °C/s ramp). Analysis of droplet samples was then performed using the QX200 Droplet Digital PCR System (Bio-Rad). We next divided the copies/μL for HDR (%): HDR (FAM) / REF (HEX). The following primers and probes were used in the ddPCR reaction:

CCR5-BGH
Forward Primer (FP): 5′-GGGAGGATTGGGAAGACA-3′
Reverse Primer (RP): 5′-AGGTGTTCAGGAGAAGGACA-3′
Probe: 5′-6-FAM/AGCAGGCATGCTGGGGATGCGGTGG/3IABkFQ-3′
CCR5-IgG1:
FP: 5′-CCTGAGCCCCGGAAAATAG-3′
RP: 5′-AGGTGTTCAGGAGAAGGACA-3′
Probe: 5′-6-FAM/AGCAGGCATGCTGGGGATGCGGTGG/3IABkFQ-3′
CCR5-IgG4:
FP: 5′-CCTCTCCCTGTCTCTGGGTA-3′
RP: 5′-AGGTGTTCAGGAGAAGGACA-3′
Probe: 5′-6-FAM/AGCAGGCATGCTGGGGATGCGGTGG/3IABkFQ-3′
CCRL2
FP: 5′- GCTGTATGAATCCAGGTCC-3′,
RP: 5′- CCTCCTGGCTGAGAAAAAG -3′
Probe: 5′- HEX/TGTTTCCTC/ZEN/CAGGATAAGGCAGCTGT/3IABkFQ -3′

INDEL analysis using ICE software

Two- or three-days following editing, cells were collected and genomic DNA was extracted using QuickExtract DNA extraction solution (Biosearch Technologies, cat.: QE09050). The following primer sequences were used to amplify the *CCR5* locus around the sgRNA cut site as previously described[51]:

FP: 5′-CAGGGAAGCTAGCAGCAAACC-3′
RP: 5′-AGACGCAAACACAGCCACC-3′

PCR products were run on a 1% agarose gel and purified using the GeneJET Gel Extraction Kit (Thermo Fisher Scientific, cat.: FERK0692). Sanger sequencing of respective PCR samples was performed using the reverse primer. Sequencing files were then used as input for INDEL frequency analysis relative to a mock, unedited sample using the online ICE CRISPR analysis tool (Synthego, Redwood City, CA, USA)[96].

Quantification of potential off-target INDELs

Potential sgRNA off-target sites were predicted using the CRISPR Off-target Sites with Mismatches, Insertions, and Deletions (COSMID) online tool[97]. Sites were ranked according to score and the predicted sites ranked 8–20 were further analyzed (top 7 sites previously analyzed)[51]. PCR amplification of these sites was performed using genomic DNA from mock-edited and sg-*CCR5* RNP-edited cells. Primers were designed around the target site and included Illumina adapters (FP adapter: 5′-ACACTCTTTCCCTACACGACGCTCTTCCGATCT-3′, RP adapter: 5′-GACTGGAGTTCAGACGTGTGCTCTTCCGATCT-3′). Sequences of the primers used can be found in Supplementary Table 5. PCR products were then purified by gel electrophoresis and subsequent extraction using the GeneJet Gel Extraction Kit (Thermo Fisher Scientific, cat.: FERK0692). Purified samples were submitted for library preparation and sequencing by Amplicon-EZ NGS (Azenta Life Sciences). Paired-end reads from the resulting NGS sequencing were then aligned to the specified off-target regions using the CRISPResso2 online tool for quantification of insertions and deletions[98].

PCR and gel electrophoresis for knock-in

Two- or three-days following editing, cells were collected and genomic DNA was extracted using QuickExtract DNA extraction solution (Biosearch Technologies, cat.: QE09050). In-out PCR was performed with 3 forward primers and one reverse primer to selectively amplify knock-in events of the Ibalizumab, 10-1074, and PGDM1400 antibody cassettes. Primers used were as follows:

Ibalizumab FP: 5′-ACAGTCCTCAGGACTCTACTCC-3′
10-1074 FP: 5′-TATGGCGTGGTGAGCTTTGG-3′
PGDM1400 FP: 5′-CTGGGACCTCCGTAAAGGTCT-3′
CCR5 RP: 5′-AGACGCAAACACAGCCACC-3′

PCR products were run on a 1% agarose gel and imaged using a Bio-Rad ChemiDoc XRS+ gel imager.

Antibody production and purification

Full length heavy and light chains for each antibody were cloned by restriction enzyme digest or Gibson Assembly (New England Biolabs) into pCMVR either individually or with a linker. Antibody constructs were expressed in Expi293F cells (Thermo Fisher Scientific, cat.: A14527) and grown in combined media (66% FreeStyle/33% Expi media, Thermo Fisher Scientific, cat.: 12338018 and A1435101, respectively) at 37 °C and 8% CO2 with shaking at 120 rpm. Antibody constructs were transfected using FectoPRO transfection reagent (Polyplus, Sébastien Brant, France, cat.: 101000014) with a transfection mixture of 10 mL of culture media, 60 μg of total DNA and 130 μL of FectoPro for each 90 mL of cell culture (for a total transfected cell culture volume of 100 mL or scaled down for 50 μg of total DNA in 75 mL total volume). Heavy and light chain plasmids were used at a 1:1 ratio, while single plasmid linker antibody constructs were used alone. For simultaneous production of a traditional and linker antibody, 20 μg of each plasmid (traditional light chain, traditional heavy chain, and linker antibody) were applied in 100 mL cell cultures. Cells were transfected at a cell density $3\text{-}4 \times 10^6$ cells/mL and harvested 4 days post-transfection by spinning at >4200 g for 15 min. Cell culture supernatants were filtered through a 0.45μm filter, combined with 1/10th volume of 10x phosphate-buffered saline (PBS) and purified using the ÄKTA pure fast performance liquid chromotography (FPLC, Cytiva) with a 5 mL MabSelect PrismA column (Cytvia, cat.: 17549802) using wash steps with 1x PBS and elution with 100 mM glycine (pH 2.8) into one-tenth volume of 1 M Tris (pH 8.0). The eluted proteins were then concentrated using 50-kDa or 100-kDa cutoff centrifugal concentrators and further purified by size exclusion on the same ÄKTA FPLC with Superdex 200 Increase 10/300 GL column (Cytiva, cat.: 28-9909-44). Proteins were then further concentrated using 50-kDa or 100-kDa cutoff centrifugal concentrators. Final concentration was determined with a NanoDrop UV-Vis spectrophotometer.

Immunophenotyping of B cells

All samples were blocked for non-specific binding with human FcR Blocking Reagent (Miltenyi Biotec, cat.: 130-059-901) for 10 min at room temperature and then stained for 30 min at 4 °C with the following antibody cocktail: anti-human CD19 (Becton, Dickinson and Company, BD, Franklin Lakes, NJ, USA, cat.: 562440), anti-human CD20 (BioLegend, San Diego, CA, USA, cat.: 302326), anti-human CD27 (BioLegend, cat.: 302832), anti-human CD38 (BD, cat.: 555462), anti-

human IgD (BioLegend, cat.: 348232), and anti-human IgM (BD, cat.: 563903). Samples were analyzed on a FACSAria II SORP (BD). Data was subsequently analyzed using FlowJo (v.10.9.0).

ELISA for antibody concentration

Antigen specific ELISA was used to determine the concentration of each HIV-inhibiting antibody in B cell supernatant. Anti-IgG Fc ELISA was used to detect human IgG in mouse serum or B cell culture supernatant. 10-1074, Ibalizumab, and total human IgG were detected using a previously described protocol[99]. Briefly, Nunc MaxiSorp 96 Well Plates (Thermo Fisher Scientific, cat.: 44-2404-21) were coated with 0.8 μg/mL recombinant $HIV_{JR\text{-}CSF}$ gp120 (for detecting 10-1074; Immune Technology, Tarrytown, NY, USA, cat.: IT-001-0025p), 1 μg/mL recombinant rhesus monkey CD4 protein (for detecting Ibalizumab; Abcam, Cambridge, UK, cat.: ab208305), or 1:100 diluted goat anti-human IgG-Fc (for detecting total human IgG; Fortis Life Sciences, Waltham, MA, USA, cat.: A80-104A) in 0.05 M carbonate-bicarbonate buffer solution (Sigma-Aldrich, cat.: C3041) for 1 hour at room temperature or overnight at 4 °C. Plates were then blocked in tris-buffered saline (TBS) with 1% bovine serum albumin (BSA; Miltenyi Biotech, cat.: 130-091-376) for 30 min. Media and serum samples were diluted in TBS with 1% BSA and 0.05% Tween-20 and incubated on the plate for 4 h at room temperature or overnight at 4 °C. Plates were then incubated with horseradish peroxidase (HRP)–conjugated goat anti-human IgG-Fc antibody (Fortis Life Sciences, cat.: A80-104A) at a 1:2500 dilution. Detection was performed with the 1-Step™ TMB Substrate Kit (Thermo Fisher Scientific, cat.: 34021) and quenched with 3 M H_2SO_4. Plates were read at 450 nm using a Molecular Devices SpectraMax M3 plate reader with SoftMax Pro software. Standard curves were created using purified versions of each HIV inhibiting antibody or purified human IgG/kappa from normal serum (Bethyl, Montgomery, TX, USA, cat.: P80-111). Results were analyzed using GraphPad Prism v10 software to calculate a standard curve using a 4-parameter or 5-parameter sigmoidal algorithm. The curve with a higher r-squared was selected and results were interpolated for each sample. PGDM1400 and CAP256V2LS were detected with a modified protocol. Briefly, recombinant HIV-1 Env trimer, BG505 SOSIP, was biotinylated with the EZ-Link™-Biotinylation Kit (Thermo Fisher Scientific, cat.: 21435) according to the manufacturer instructions[100]. Nunc MaxiSorp plates were coated with 4 μg/mL streptavidin (Thermo Fisher Scientific, cat.: PI21122) in PBS at room temperature for 1 hour. Plates were then blocked with ChonBlock (Thermo Fisher Scientific, cat.: 50-152-6971) overnight at 4 °C. The next day, 1 μg/mL biotinylated BG505 SOSIP trimer was added for 1 hour at room temperature. Samples were diluted in PBS with 0.1% BSA and 0.05% Tween-20 and incubated on the coated plates for 1 hour. Plates were then detected with HRP-conjugated anti-human IgG-Fc antibody as described above. Results were analyzed as described above.

Total protein gel stain of purified antibodies

Purified antibodies (0.5 μg each) were denatured by adding 4X Laemmli sample buffer (Bio-Rad, cat.: 1610747) and 2-mercaptoethanol and heating at 100 °C for 5 min. Samples were loaded onto a 4–15% Mini-PROTEAN TGX precast protein gel (Bio-Rad, cat.: 4561084). Following electrophoresis, gel was fixed by incubation in 100 mL of 50% methanol, 7% acetic acid and agitated on an orbital shaker for 30 min, twice. Following fixation, gel was stained with of SYPRO Ruby gel stain (Invitrogen, cat.: S12000) on an orbital shaker overnight at room temperature. The following day, the gel was washed once in 100 mL of 10% methanol, 7% acetic acid for 30 min, followed by two washes in ultrapure water for 5 minutes each. The gel was then imaged using a Bio-Rad ChemiDoc XRS+ gel imager using ImageLab software.

Western blotting of purified antibodies

Purified antibodies (0.5 μg each) were denatured by adding 4X Laemmli sample buffer (Bio-Rad, cat.: 1610747) and 2-mercaptoethanol and heating at 100 °C for 5 min. Samples were loaded onto a 4–15% Mini-PROTEAN TGX precast protein gel (Bio-Rad, cat.: 4561084). Following electrophoresis, protein from gel was transferred to a PVDF membrane using the Trans-Blot Turbo Transfer System (Bio-Rad, cat.: 1704150). Subsequently, the membrane was blocked using Blotting-Grade Blocker (Bio-Rad, cat.: 1706404) in phosphate-buffered saline with 0.02% Tween 20 (PBS-T) for 30 min at room temperature. Membrane was then incubated in 1:5000 primary antibody (HRP-conjugated Goat pAb to human IgG, Abcam, cat.: 7153) overnight at 4 °C. The next day, the membrane was washed three times with PBS-T. SuperSignal™ West Pico PLUS Chemiluminescent Substrate (Thermo Fisher Scientific, cat.: 34579) was used for detection and blots were imaged using a Bio-Rad ChemiDoc XRS+ gel imager using ImageLab software.

Mass spectrometry for antibody pairing

Individual samples were analyzed by liquid chromatography-electrospray ionization-mass spectrometry (LC-ESI/MS) on the Waters Acquity UPLC (Waters Corporation, Milford, MA) and Thermo Exploris 240 Orbitrap BioPharma mass spectrometer using two chromatographic methods. For concentrated antibodies produced in Expi293F cells, the column was a Waters MassPREP 5 × 2.1 mm diphenyl desalting column maintained (Waters Corporation, cat.: 186004032) at 50 °C with flow rate 0.2 mL/min. The injection volume was 3 μL. The initial solvent conditions were 95:5 water (A) / acetonitrile (B) both with 0.1% formic acid held for 2.5 min, ramped to 95% B at 4 min then held for 2 min. Four samples were processed for this experiment. (1) Control intact mass monoclonal antibody standard (Intact mAb Mass Check Standard; Waters Corporation, cat.: 186006552). (2) Individually produced and purified S2-4 antibody. (3) Individually produced and purified Linker 10-1074 antibody. (4) Combined S2-4 and Linker 10-1074 production and purification. A single replicate was used for each experiment. For antibodies isolated from B cell culture supernatant, the column was a Waters BioResolve RP mAb Polyphenyl 450 A 2.7 u 2.1 × 100 mm (Waters Corporation, cat.: 186008945), maintained at 80 °C with flow rate 0.25 mL/min. The injection volume was 3 μL. The initial solvent conditions were 75:25 water (A)/acetonitrile (B) both with 0.1% formic acid held for 2 min, ramped to 55% B at 20 min then to 80% B at 22 min. (1) Control intact mass monoclonal antibody standard (Intact mAb Mass Check Standard; Waters Corporation, cat.: 186006552). (2) Combined S2-4 and Linker 10-1074 production and purification. (3) Purified antibody from mock edited B cells. (4). Purified antibody from Linker 10-1074 edited B cells. A single replicate was used for each experiment. For both experiments, mass spectra were collected in positive full scan MS mode with Orbitrap resolution 30000, mass range 1500–5000 Da, RF lens 100 V, and Source Fragmentation Energy 80 V. PMI-Byonic (RRID:SCR_016735) Intact software v4.5-53-g1f2b882c4e x64 from Protein Metrics was used to generate deconvoluted mass spectra.

TZM-bl infection assay for determining IC_{50}

The TZM-bl HIV-1 pseudotype infection assay was adapted from previously described protocols[101,102]. TZM-bl cells were obtained through the NIH AIDS Reagent Program (cat.: 8129) and cultured in DMEM with 10% BGS, and 1% penicillin-streptomycin (complete DMEM) at 37 °C, 5% CO2, and ambient oxygen levels. HIV-1 env pseudotyped lentivirus was produced as previously described using a pNL4-3ΔEnvGFP backbone plasmid and *env* plasmids provided by the NIH AIDS Reagents Program (cat.: 11100 and cat.: 12670, respectively)[103]. Briefly, 5×10^3 cells were plated in black-walled, clear-bottom 96-well plates (Corning, Corning, NY, USA, cat.: 07-200-565) and incubated overnight. The next day, each antibody was incubated with HIV-1 pseudovirus for 1 hour at 37 °C at concentrations from 5 μg/mL to 5×10^{-5} μg/mL using 10-fold serial dilution in complete DMEM with 15 μg/mL DEAE-dextran (Sigma-Aldrich, D9885). Culture media was aspirated from the TZM-bl cells and replaced with antibody-virus mixture. Virus only (no antibodies added) and cells only (no virus or antibodies) wells were included for

determining 100% and 0% infection readouts. Cells were incubated for 48 h then measured for luciferase signal corresponding to infection. Briefly, cells were lysed with Reporter Lysis Buffer (Promega, Madison, WI, USA, cat.: E3971) and freeze-thawed at −80 °C. Lysed samples were read for relative luminescence units (RLU) using a Synergy H1 plate reader (BioTek, Winooski, VT, USA) that automatically injected luciferin solution consisting of the following: 200 mM Tris [pH 8], 10 mM MgCl2, 300 μM ATP, Firefly Luciferase Signal Enhancer (Thermo Fischer Scientific, cat. 16180), and 150 μg/mL d-luciferin (Biosynth Chemistry & Biology, Staad, Switzerland, cat.: L8220). Percent infection was determined by normalizing RLU values to the average RLU of virus-only and cells-only wells using GraphPad Prism v10. IC_{50} was calculated using a linear regression dose-response curve fit for inhibitor versus response (three parameters) based on the average of technical duplicate wells using GraphPad Prism v10.

TZM-bl infection assay with B cell supernatant

Six days post-editing, B cells were plated at 1×10^6 cells/mL and antibody was allowed to accumulate in supernatant for five days. Culture supernatant was collected following centrifugation to remove cells. A modified TZM-bl assay was performed as described above with the following changes. Culture supernatant was diluted in complete DMEM with two-fold serial dilutions. Then, 50 μL of each dilution was mixed with 50 μL of HIV-1 pseudovirus + complete DMEM for final dilutions of culture media ranging from 1:2 to 1:4096 and a final concentration of 15 μg/mL DEAE-dextran (Sigma-Aldrich, cat.: D9885). Samples were incubated for 1 h at 37 °C before being applied to TZM-bl cells. Luciferase readout was measured as described above. Analysis was performed by normalizing the luciferase signal to the corresponding well receiving mock-edited B cell media. Best fit lines and media IC_{50} was calculated using a linear regression dose-response curve fit for inhibitor versus response (three parameters) based on the average of technical duplicate wells using GraphPad Prism v10.

Colony forming unit (CFU) assay and colony genotyping

Two days post-electroporation 500 HSPCs were plated in each well of a SmartDish 6-well plate (STEMCELL Technologies, Vancouver, Canada, cat.: 27370) containing MethoCult H4434 Classic (STEMCELL Technologies, cat.: 04444). After 14 days, the wells were imaged using the STEMvision Hematopoietic Colony Counter (STEMCELL Technologies). Colonies were counted and scored with manual correction to determine the number of BFU-E, CFU-GM, and CFU-GEMM colonies. Individual colonies were picked and gDNA was extracted using QuickExtract DNA extraction solution (Biosearch Technologies, cat.: QE09050). Knock-in was determined by ddPCR and INDELs were determined by ICE analysis as described above.

Mouse models

NOD.Cg-Prkdc^{scid}Il2rg^{tm1Wjl}/SzJ (NSG) and NOD.Cg-*Kit*$^{W-41J}$*Tyr*$^{+}$*Prkdc*^{scid} *Il2rg*^{tm1Wjl}/ThomJ (NBSGW) mice were purchased from Jackson Laboratories (Bar Harbor, ME, USA). 20 NSG mice were used in this work, including 10 males and 10 females. 12 NBSGW mice were used in this work, including 6 males and 6 females. Mice were housed in the Stanford University barrier facility with a 12/12-h light/dark cycle at an ambient temperature of 22 °C and with 50% humidity. All experiments were completed under the Administrative Panel on Laboratory Animal Care (APLAC Protocol #25065).

CD34^{+} HSPC transplantation into immunodeficient mice

For the experiment in NSG mice, 6–8 week old mice were irradiated with 2 Gy approximately 4 h prior to transplantation. 8.5×10^5 mock or gene-edited cells were transplanted into each mouse via retro-orbital injection. For the experiment in NBSGW mice, 6–8 week old mice received no conditioning and 5×10^5 mock or gene-edited cells were transplanted into each mouse via retro-orbital injection.

Assessment of human HSPC engraftment

Human engraftment was assessed at 12- (NBSGW) or 16-weeks (NSG) post-transplantation. Mice were euthanized and bone marrow and spleen were harvested from recipient mice. Mononuclear cells from bone marrow samples were isolated via Ficoll gradient centrifugation. Spleen samples were treated with RBC Lysis Buffer (IBI Scientific, Dubuque, IA, USA, cat.: IB47620) to eliminate mature red blood cells. All samples were blocked for non-specific binding with FcR Blocking Reagent for human (Miltenyi Biotec, cat.: 130-059-901) and mouse (Miltenyi Biotec, cat.: 130-092-575) for 10 min at room temperature and then stained for 30 min at 4 °C with the following antibody cocktail: anti-mouse CD45.1 (Biolegend, cat.: 110735), anti-mouse TER-119 (eBiosciences, San Diego, CA, USA, cat.: 15-5921-82), anti-human CD45 (Biolegend, cat.: 368540), anti-human HLA-ABC (Biolegend, cat. 311426), anti-human CD33 (BD, cat.: 555450), anti-human CD19 (Biolegend, cat.: 302212), anti-human CD3 (Biolegend, cat.: 300328), and viability dye Ghost Dye™ Violet 540 (Tonbo Bioscience, San Diego, CA, USA, cat. 130879T100). Samples were analyzed on a CytoFLEX flow cytometer (Beckman-Coulter, Indianapolis, IN, USA). Data was subsequently analyzed using FlowJo (v.10.9.0). Humam CD19^{+} cells were isolated from the bone marrow using positive selection with the CD19 MicroBeads, human kit (Miltenyi Biotec, cat.: 130-050-301). Knock-in and INDEL frequencies were determined by ddPCR and ICE analysis as described above.

Statistics and reproducibility

All statistical analysis was performed using GraphPad Prism v10 software. In general, two or more biological donors were used for most experiments using primary cells, with specific numbers indicated in individual figure legends. No data were excluded from the analysis except where specifically noted below due to technical error resulting in loss of sample or insufficient sample amount to generate reliable data. Excluded data points include a single NSG mouse engrafted with Ibalizumab-edited cells due to mortality within 1-week of irradiation (Fig. 3), one spleen sample from each NSG mouse treatment group due to coagulation that prevented analysis (Fig. 3), one serum sample from an NSG mouse engrafted with mock cells due to failed collection (Supplementary Fig. 7a), and two W41 mouse bone marrow samples for construct-specific ddPCR due to insufficient genomic DNA concentration (Supplementary Fig. 6c). Mouse numbers were determined based on availability of mice and primary cells. The resulting data were sufficient to show significance of differences between groups where important. No statistical method was used to predetermine sample size. A similar number of male and female mice was maintained for each treatment group. The sex distribution was not incorporated into the analysis. Sex information is disaggregated in the source data. Randomization was not applicable in the reported experiments. The investigators were not blinded to allocation during experiments and outcome assessment.

Reporting summary

Further information on research design is available in the Nature Portfolio Reporting Summary linked to this article.

Data availability

Reagents and protocols are available upon request from the corresponding author. The mass spectrometry data generated in this study have been deposited in the MassIVE database under accession code MSV000096716 [https://massive.ucsd.edu/ProteoSAFe/dataset.jsp?task=7ef9f7d4aa18459daf5139a098b0215b]. High-throughput NGS sequencing data generated for off-target INDEL analysis is available through the NCBI Sequence Read Archive database under accession code PRJNA1199503. Source data are provided with this paper.

References

1. Joint United Nations Programme on HIV/AIDS. *The path that ends AIDS: UNAIDS Global AIDS Update 2023*. UNAIDS repor (Joint United Nations Programme on HIV/AIDS, 2023).
2. Teeraananchai, S., Kerr, S., Amin, J., Ruxrungtham, K. & Law, M. Life expectancy of HIV-positive people after starting combination antiretroviral therapy: a meta-analysis. *HIV Med.* **18**, 256–266 (2017).
3. Gandhi, R. T. et al. Antiretroviral drugs for treatment and prevention of HIV infection in adults. *JAMA* **329**, 63 (2023).
4. Paterson, D. L. et al. Adherence to protease inhibitor therapy and outcomes in patients with HIV infection. *Ann. Intern. Med.* **133**, 21–30 (2000).
5. Barbara, T. Adherence to antiretroviral therapy by human immunodeficiency virus–infected patients. *J. Infect. Dis.* **185**, S143–S151 (2002).
6. Kim, J., Lee, E., Park, B.-J., Bang, J. H. & Lee, J. Y. Adherence to antiretroviral therapy and factors affecting low medication adherence among incident HIV-infected individuals during 2009–2016: a nationwide study. *Sci. Rep.* **8**, https://doi.org/10.1038/s41598-018-21081-x (2018).
7. Chun, T. W. et al. Presence of an inducible HIV-1 latent reservoir during highly active antiretroviral therapy. *Proc. Natl. Acad. Sci. USA* **94**, 13193–13197 (1997).
8. Finzi, D. et al. Identification of a reservoir for HIV-1 in patients on highly active antiretroviral therapy. *Science* **278**, 1295 (1997).
9. Mahomed, S., Garrett, N., Baxter, C., Abdool Karim, Q. & Abdool Karim, S. S. Clinical trials of broadly neutralizing monoclonal antibodies for human immunodeficiency virus prevention: a review. *J. Infect. Dis.* **223**, 370–380 (2021).
10. Frattari, G. S., Caskey, M. & Søgaard, O. S. Broadly neutralizing antibodies for HIV treatment and cure approaches. *Curr. Opin. HIV AIDS* **18**, 157–163 (2023).
11. Markham, A. Ibalizumab: first global approval. *Drugs* **78**, 781–785 (2018).
12. Pace, C. S. et al. Anti-CD4 monoclonal antibody ibalizumab exhibits breadth and potency against HIV-1, with natural resistance mediated by the loss of a V5 Glycan in Envelope. *JAIDS J. Acquir. Immune Deficiency Syndromes* **62**, 1–9 (2013).
13. Boon, L. Development of anti-CD4 MAb hu5A8 for treatment of HIV-1 infection: preclinical assessment in non-human primates. *Toxicology* **172**, 191–203 (2002).
14. Emu, B. et al. Phase 3 study of Ibalizumab for Multidrug-Resistant HIV-1. *N. Engl. J. Med.* **379**, 645–654 (2018).
15. Sok, D. & Burton, D. R. Recent progress in broadly neutralizing antibodies to HIV. *Nat. Immunol.* **19**, 1179–1188 (2018).
16. Caskey, M. Broadly neutralizing antibodies for the treatment and prevention of HIV infection. *Curr. Opin. HIV AIDS* **15**, 49–55 (2020).
17. Mendoza, P. et al. Combination therapy with anti-HIV-1 antibodies maintains viral suppression. *Nature* **561**, 479–484 (2018).
18. Gaebler, C. et al. Prolonged viral suppression with anti-HIV-1 antibody therapy. *Nature*, https://doi.org/10.1038/s41586-022-04597-1 (2022).
19. Julg, B. et al. Safety and antiviral activity of triple combination broadly neutralizing monoclonal antibody therapy against HIV-1: a phase 1 clinical trial. *Nat. Med.* **28**, 1288–1296 (2022).
20. Badamchi-Zadeh, A. et al. Therapeutic efficacy of Vectored PGT121 gene delivery in HIV-1-Infected humanized mice. *J. Virol.* **92**, https://doi.org/10.1128/JVI.01925-17 (2018).
21. van den Berg, F. T. et al. AAV-Mediated expression of broadly neutralizing and vaccine-like antibodies targeting the HIV-1 envelope V2 Region. *Mol. Ther. Methods Clin. Dev.* **14**, 100–112 (2019).
22. Martinez-Navio, J. M. et al. Adeno-associated virus delivery of Anti-HIV monoclonal antibodies can drive long-term virologic suppression. *Immunity* **50**, 567–575.e565 (2019).
23. Martinez-Navio, J. M. et al. Long-term delivery of an Anti-SIV monoclonal antibody with AAV. *Front. Immunol.* **11**, 449 (2020).
24. Casazza, J. P. et al. Safety and tolerability of AAV8 delivery of a broadly neutralizing antibody in adults living with HIV: a phase 1, dose-escalation trial. *Nat. Med.* **28**, 1022–1030 (2022).
25. Joshi, L. R., Gálvez, N. M. S., Ghosh, S., Weiner, D. B. & Balazs, A. B. Delivery platforms for broadly neutralizing antibodies. *Curr. Opin. HIV AIDS* **18**, 191–208 (2023).
26. Klamroth, R. et al. Global Seroprevalence of Pre-existing Immunity Against AAV5 and Other AAV Serotypes in People with Hemophilia A. *Hum. Gene Ther.* **33**, 432–441 (2022).
27. Priddy, F. H. et al. Adeno-associated virus vectored immunoprophylaxis to prevent HIV in healthy adults: a phase 1 randomised controlled trial. *Lancet HIV* **6**, e230–e239 (2019).
28. Hung, K. L. et al. Engineering protein-secreting plasma cells by homology-directed repair in primary human B cells. *Mol. Ther.* **26**, 456–467 (2018).
29. Moffett, H. F. et al. B cells engineered to express pathogen-specific antibodies protect against infection. *Sci. Immunol.* **4**, eaax0644 (2019).
30. Hartweger, H. et al. HIV-specific humoral immune responses by CRISPR/Cas9-edited B cells. *J. Exp. Med.* **216**, 1301–1310 (2019).
31. Nahmad, A. D. et al. Engineered B cells expressing an anti-HIV antibody enable memory retention, isotype switching and clonal expansion. *Nat. Commun.* **11**, 5851 (2020).
32. Huang, D. et al. Vaccine elicitation of HIV broadly neutralizing antibodies from engineered B cells. *Nat. Commun.* **11**, 5850 (2020).
33. Hütter, G. et al. Long-Term control of HIV byCCR5Delta32/Delta32 stem-cell transplantation. *N. Engl. J. Med.* **360**, 692–698 (2009).
34. Gupta, R. K. et al. HIV-1 remission following CCR5Δ32/Δ32 haematopoietic stem-cell transplantation. *Nature* **568**, 244–248 (2019).
35. Jensen, B.-E. O. et al. In-depth virological and immunological characterization of HIV-1 cure after CCR5Δ32/Δ32 allogeneic hematopoietic stem cell transplantation. *Nat. Med.* **29**, 583–587 (2023).
36. Solloch, U. V. et al. Frequencies of gene variant CCR5-Δ32 in 87 countries based on next-generation sequencing of 1.3 million individuals sampled from 3 national DKMS donor centers. *Hum. Immunol.* **78**, 710–717 (2017).
37. Gragert, L. et al. HLA Match likelihoods for hematopoietic stem-cell grafts in the U.S. Registry. *N. Engl. J. Med.* **371**, 339–348 (2014).
38. Styczyński, J. et al. Death after hematopoietic stem cell transplantation: changes over calendar year time, infections and associated factors. *Bone Marrow Transplant.* **55**, 126–136 (2020).
39. Kordelas, L., Verheyen, J. & Esser, S. Shift of HIV tropism in stem-cell transplantation with CCR5 Delta32 mutation. *N. Engl. J. Med.* **371**, 880–882 (2014).
40. Brumme, Z. L. et al. Molecular and clinical epidemiology of CXCR4-using HIV-1 in a large population of antiretroviral-naive individuals. *J. Infect. Dis.* **192**, 466–474 (2005).
41. Shepherd, J. et al. Emergence and persistence of CXCR4-tropic HIV-1 in a population of men from the multicenter AIDS cohort study. *J. Infect. Dis.* **198**, 1104–1112 (2008).
42. Xu, L. et al. CRISPR-Edited stem cells in a patient with HIV and acute lymphocytic leukemia. *N. Engl. J. Med.* **381**, 1240–1247 (2019).
43. DiGiusto, D. L. et al. Preclinical development and qualification of ZFN-mediated CCR5 disruption in human hematopoietic stem/progenitor cells. *Mol. Ther. Methods Clin. Dev.* **3**, 16067–16067 (2016).
44. Burke, B. P. et al. Engineering cellular resistance to HIV-1 infection in vivo using a dual therapeutic lentiviral vector. *Mol. Ther. Nucleic Acids* **4**, e236 (2015).

45. Luo, X. M. et al. Engineering human hematopoietic stem/progenitor cells to produce a broadly neutralizing anti-HIV antibody after in vitro maturation to human B lymphocytes. *Blood* **113**, 1422–1431 (2009).
46. Kuhlmann, A.-S. et al. Long-term persistence of Anti-HIV broadly neutralizing antibody-secreting hematopoietic cells in humanized mice. *Mol. Ther.* **27**, 164–177 (2019).
47. Wolstein, O. et al. Preclinical safety and efficacy of an anti–HIV-1 lentiviral vector containing a short hairpin RNA to CCR5 and the C46 fusion inhibitor. *Mol. Ther. Methods Clini. Dev.* **1,** e11 (2014).
48. Ringpis, G.-E. E. et al. Engineering HIV-1-resistant T-cells from short-hairpin RNA-expressing hematopoietic stem/progenitor cells in humanized BLT mice. *PloS ONE* **7**, e53492 (2012).
49. Themis, M. et al. Oncogenesis following delivery of a nonprimate lentiviral gene therapy vector to fetal and neonatal mice. *Mol. Ther.* **12**, 763–771 (2005).
50. Philippidis, A. CASGEVY makes history as FDA Approves First CRISPR/Cas9 genome edited therapy. *Human Gene Ther.* **35**, 1–4 (2024).
51. Dudek, A. M. et al. A simultaneous knockout knockin genome editing strategy in HSPCs potently inhibits CCR5- and CXCR4-tropic HIV-1 infection. *Cell Stem Cell* **31**, 499–518.e496 (2024).
52. Caskey, M. et al. Antibody 10-1074 suppresses viremia in HIV-1-infected individuals. *Nat. Med.* **23**, 185–191 (2017).
53. Sok, D. et al. Recombinant HIV envelope trimer selects for quaternary-dependent antibodies targeting the trimer apex. *Proc. Natl. Acad. Sci. USA* **111**, 17624–17629 (2014).
54. Zhang, B. et al. Engineering of HIV-1 neutralizing antibody CAP256V2LS for manufacturability and improved half life. *Sci. Rep.* **12**, https://doi.org/10.1038/s41598-022-22435-2 (2022).
55. Caskey, M. et al. Viraemia suppressed in HIV-1-infected humans by broadly neutralizing antibody 3BNC117. *Nature* **522**, 487–491 (2015).
56. Schommers, P. et al. Restriction of HIV-1 escape by a highly broad and potent neutralizing antibody. *Cell* **180**, 471–489.e422 (2020).
57. Koerber, J. T., Hornsby, M. J. & Wells, J. A. An improved single-chain Fab platform for efficient display and recombinant expression. *J. Mol. Biol.* **427**, 576–586 (2015).
58. deCamp, A. et al. Global panel of HIV-1 Env reference strains for standardized assessments of vaccine-elicited neutralizing antibodies. *J. Virol.* **88**, 2489–2507 (2014).
59. Yoon, H. et al. CATNAP: a tool to compile, analyze and tally neutralizing antibody panels. *Nucleic Acids Res.* **43**, W213–W219 (2015).
60. Vakulskas, C. A. et al. A high-fidelity Cas9 mutant delivered as a ribonucleoprotein complex enables efficient gene editing in human hematopoietic stem and progenitor cells. *Nat. Med.* **24**, 1216–1224 (2018).
61. Selvaraj, S. et al. High-efficiency transgene integration by homology-directed repair in human primary cells using DNA-PKcs inhibition. *Nat. Biotechnol.* https://doi.org/10.1038/s41587-023-01888-4 (2023).
62. Dever, D. P. et al. CRISPR/Cas9 β-globin gene targeting in human haematopoietic stem cells. *Nature* **539**, 384–389 (2016).
63. Gomez-Ospina, N. et al. Human genome-edited hematopoietic stem cells phenotypically correct Mucopolysaccharidosis type I. *Nat. Commun.* **10**, https://doi.org/10.1038/s41467-019-11962-8 (2019).
64. Cromer, M. K. et al. Gene replacement of α-globin with β-globin restores hemoglobin balance in β-thalassemia-derived hematopoietic stem and progenitor cells. *Nat. Med.* **27**, 677–687 (2021).
65. Vavassori, V. et al. Lipid nanoparticles allow efficient and harmless ex vivo gene editing of human hematopoietic cells. *Blood* **142**, 812–826 (2023).
66. DeWitt, M. A. et al. Selection-free genome editing of the sickle mutation in human adult hematopoietic stem/progenitor cells. *Sci. Transl. Med.* **8**, 360ra134 (2016).
67. Genovese, P. et al. Targeted genome editing in human repopulating haematopoietic stem cells. *Nature* **510**, 235–240 (2014).
68. Lattanzi, A. et al. Development of β-globin gene correction in human hematopoietic stem cells as a potential durable treatment for sickle cell disease. *Sci. Transl. Med.* **13**, https://doi.org/10.1126/scitranslmed.abf2444 (2021).
69. Xu, L. et al. Molecular dynamics of genome editing with CRISPR-Cas9 and rAAV6 virus in human HSPCs to treat sickle cell disease. *Mol. Ther. Methods Clin. Dev.* **30**, 317–331 (2023).
70. Vuyyuru, R., Patton, J. & Manser, T. Human immune system mice: current potential and limitations for translational research on human antibody responses. *Immunol. Res.* **51**, 257–266 (2011).
71. Jangalwe, S., Shultz, L. D., Mathew, A. & Brehm, M. A. Improved B cell development in humanized NOD-scid IL2Rγ(null) mice transgenically expressing human stem cell factor, granulocyte-macrophage colony-stimulating factor and interleukin-3. *Immunity Inflamm. Dis.* **4**, 427–440 (2016).
72. Audigé, A. et al. Long-term leukocyte reconstitution in NSG mice transplanted with human cord blood hematopoietic stem and progenitor cells. *BMC Immunol.* **18**, 28 (2017).
73. Choi, B. et al. Human B cell development and antibody production in humanized NOD/SCID/IL-2Rγnull (NSG) mice conditioned by Busulfan. *J. Clin. Immunol.* **31**, 253–264 (2011).
74. Velounias, R. L. & Tull, T. J. Human B-cell subset identification and changes in inflammatory diseases. *Clin. Exp. Immunol.* **210**, 201–216 (2022).
75. Brewer, R. C. et al. BNT162b2 vaccine induces divergent B cell responses to SARS-CoV-2 S1 and S2. *Nat. Immunol.* **23**, 33–39 (2022).
76. Leonard, A. & Tisdale, J. F. A new frontier: FDA approvals for gene therapy in sickle cell disease. *Mol. Ther.* **32**, 264–267 (2024).
77. Dudek, A. M. & Porteus, M. H. Answered and unanswered questions in early-stage viral vector transduction biology and innate primary cell toxicity for ex-vivo gene editing. *Front. Immunol.* **12**, 660302 (2021).
78. Baik, R. et al. Transient inhibition of 53BP1 increases the frequency of targeted integration in human hematopoietic stem and progenitor cells. *Nat. Commun.* **15**, 111 (2024).
79. Schiroli, G. et al. Precise gene editing preserves hematopoietic stem cell function following transient p53-Mediated DNA damage response. *Cell Stem Cell* **24**, 551–565.e558 (2019).
80. Kamboj, M. & Shah, M. K. Vaccination of the stem cell transplant recipient and the hematologic malignancy patient. *Infect. Dis. Clin. North Am.* **33**, 593–609 (2019).
81. Goh, J. B. & Ng, S. K. Impact of host cell line choice on glycan profile. *Crit. Rev. Biotechnol.* **38**, 851–867 (2018).
82. Gardner, M. R. et al. Anti-drug antibody responses impair prophylaxis mediated by AAV-Delivered HIV-1 broadly neutralizing antibodies. *Mol. Ther.* **27**, 650–660 (2019).
83. Seaman, M. S. et al. Optimization and qualification of a functional anti-drug antibody assay for HIV-1 bnAbs. *J. Immunol. Methods* **479**, 112736 (2020).
84. Abès, R. & Teillaud, J.-L. Impact of Glycosylation on effector functions of therapeutic IgG. *Pharmaceuticals* **3**, 146–157 (2010).
85. Liu, L. Antibody glycosylation and its impact on the pharmacokinetics and pharmacodynamics of monoclonal antibodies and Fc-Fusion proteins. *J. Pharm. Sci.* **104**, 1866–1884 (2015).
86. Tristán-Manzano, M. et al. Externally-controlled systems for immunotherapy: from bench to bedside. *Front. Immunol.* **11**, 2044 (2020).

87. Yesbolatova, A. et al. The auxin-inducible degron 2 technology provides sharp degradation control in yeast, mammalian cells, and mice. *Nat. Commun.* **11**, 5701 (2020).
88. Macdonald, L. et al. Rapid and specific degradation of endogenous proteins in mouse models using auxin-inducible degrons. *eLife* **11**, e77987 (2022).
89. Mercer, J. A. et al. Continuous evolution of compact protein degradation tags regulated by selective molecular glues. *Science* **383**, eadk4422 (2024).
90. Martin, R. M. et al. Improving the safety of human pluripotent stem cell therapies using genome-edited orthogonal safeguards. *Nat. Commun.* **11**, 2713 (2020).
91. Sahillioglu, A. C. & Schumacher, T. N. Safety switches for adoptive cell therapy. *Curr. Opin. Immunol.* **74**, 190–198 (2022).
92. Aurnhammer, C. et al. Universal real-time PCR for the detection and quantification of adeno-associated virus serotype 2-derived inverted terminal repeat sequences. *Hum. Gene Ther. Methods* **23**, 18–28 (2012).
93. Bak, R. O., Dever, D. P. & Porteus, M. H. CRISPR/Cas9 genome editing in human hematopoietic stem cells. *Nat. Protoc.* **13**, 358–376 (2018).
94. Hendel, A. et al. Chemically modified guide RNAs enhance CRISPR-Cas genome editing in human primary cells. *Nat. Biotechnol.* **33**, 985–989 (2015).
95. Rogers, G. L. et al. Optimization of AAV6 transduction enhances site-specific genome editing of primary human lymphocytes. *Mol. Ther. Methods Clin. Dev.* **23**, 198–209 (2021).
96. Conant, D. et al. Inference of CRISPR Edits from Sanger Trace Data. *Crispr J.* **5**, 123–130 (2022).
97. Cradick, T. J., Qiu, P., Lee, C. M., Fine, E. J. & Bao, G. COSMID: a web-based tool for identifying and validating CRISPR/Cas Off-target Sites. *Mol. Ther. Nucleic Acids* **3**, e214 (2014).
98. Clement, K. et al. CRISPResso2 provides accurate and rapid genome editing sequence analysis. *Nat. Biotechnol.* **37**, 224–226 (2019).
99. Brady, J. M. et al. Antibody-mediated prevention of vaginal HIV transmission is dictated by IgG subclass in humanized mice. *Sci. Transl. Med.* **14**, eabn9662 (2022).
100. Dam, K.-M. A., Mutia, P. S. & Bjorkman, P. J. Comparing methods for immobilizing HIV-1 SOSIPs in ELISAs that evaluate antibody binding. *Sci. Rep.* **12**, 11172 (2022).
101. Montefiori, D. C. Measuring HIV neutralization in a luciferase reporter gene assay. *HIV Protoc.* **485**, 395–405 (2009).
102. Sarzotti-Kelsoe, M. et al. Optimization and validation of the TZM-bl assay for standardized assessments of neutralizing antibodies against HIV-1. *J. Immunol. Methods* **409**, 131–146 (2014).
103. Li, M. et al. Human immunodeficiency virus type 1 env clones from acute and early subtype B infections for standardized assessments of vaccine-elicited neutralizing antibodies. *J. Virol.* **79**, 10108–10125 (2005).

Acknowledgements

We thank Dr. Peter Kim for technical advice and support in purifying and testing antibodies. We thank Dr. Christopher Barnes for technical advice and for providing the BG505 SOSIP Trimer. We thank Dr. Alejandro Balazs for assistance with the gp120 ELISA. We thank the NIH AIDS Reagent Repository for providing the *env* plasmids for the panel of HIV-1 pseudoviruses. We thank the Stanford Institute for Stem Cell Biology and Regenerative Medicine FACS Core for their support and access to flow cytometry machines. We thank the Binns Program for Cord Blood Research for providing purified cord blood HSPCs. This work utilized the Thermo Exploris 240 LC/MS system (RRID:SCR_022216) that was purchased with funding from Stanford C-ShaRP (RRID:SCR_022986) and was supported by Stanford University Mass Spectrometry (RRID:SCR_017801). W.N.F. was supported by the Stanford T32 Graduate Training Program in Stem Cell Biology and Regenerative Medicine (5T32GM119995) and the Blavatnik Family Foundation as a Blavatnik Fellow. S.E.L. was supported by the Stanford Medical Scholars Research Program, the American Society of Hematology Minority Medical Student Award Program, and the Stanford Medical Scientist Training Program. M.V.F.I. was supported by the Stanford Medical Scientist Training Program (5T32GM007365) and the Ruth L Kirschstein Individual Predoctoral NRSA awarded by the NIH/NIAID (5F30AI152943). T.U.J.B. was supported by the Knight-Hennessy Graduate Scholarship and a Canadian Institutes of Health Research Doctoral Foreign Study Award (FRN:170770). A.M.D. was supported by NIH F32 Individual Postdoctoral Fellowship (1F32HL154667-01),NIH K99/R00 Pathway to Independence Award (1K99HL172253-01), and HIV Accessory and Regulatory Complexes Center Collaborative Developmental Award (NIH Parent AI170792). M.H.P. was supported by the Sutardja Chuk Professorship in Definitive and Curative Medicine and the Laurie Kraus Lacob Translational Medicine endowment.

Author contributions

W.N.F., S.E.L., K.B.E., M.V.F.I., T.U.J.B., A.U., H.Y.G., T.M.M., and A.M.D. contributed to experimental design, performance, and analysis. A.A. and N.M.J. performed experiments for in vivo engraftment studies. B.J.L. contributed to the design and direction of the project. W.N.F., S.E.L., and M.H.P. wrote the draft and finalized versions of the manuscript with input from other authors. A.M.D. and M.H.P. supervised the project.

Competing interests

M.H.P. serves on the scientific advisory board of Allogene Tx and is an advisor to Versant Ventures. M.H.P. has equity in CRISPR Tx and has equity and is a founder of Kamau Therapeutics. M.H.P., W.N.F., and S.E.L. are inventors on a provisional patent application submitted by The Board of Trustees of the Leland Stanford Junior University to the United States Patent and Trademark Office pertaining to the genetic engineering of cells for section of therapeutic antibodies (application number 63/561,249). The remaining authors declare no competing interests.

Additional information

Supplementary information The online version contains supplementary material available at https://doi.org/10.1038/s41467-025-58371-8.

Correspondence and requests for materials should be addressed to Amanda M. Dudek or Matthew H. Porteus.

Peer review information *Nature Communications* thanks the anonymous reviewers for their contribution to the peer review of this work. A peer review file is available.